FTPI-MINN-08/24; UMN-TH-2703/08

Confinement and Localization on Domain Walls

R. Auzzi[(1)], S. Bolognesi[(2)], M. Shifman [(2,3)] and A. Yung[(2,4)]

[(1)] *Department of Physics, Swansea University, Singleton Park, Swansea SA2 8PP, U.K.*

[(2)] *William I. Fine Theoretical Physics Institute, University of Minnesota, 116 Church St. S.E., Minneapolis, MN 55455, USA*

[(3)] *Laboratoire de Physique Théorique[1] Université de Paris-Sud XI Bâtiment 210, F-91405 Orsay Cédex, FRANCE*

[(4)] *Petersburg Nuclear Physics Institute, Gatchina, St. Petersburg 188300, RUSSIA and Institute of Theoretical and Experimental Physics, Moscow 117259, RUSSIA*

Abstract

We continue the studies of localization of the U(1) gauge fields on domain walls. Depending on dynamics of the bulk theory the gauge field localized on the domain wall can be either in the Coulomb phase or squeezed into flux tubes implying (Abelian) confinement of probe charges on the wall along the wall surface. First, we consider a simple toy model with one flavor in the bulk at weak coupling (a minimal model) realizing the latter scenario. We then suggest a model presenting an extension of the Seiberg–Witten theory which is at strong coupling, but all theoretical constructions are under full control if we base our analysis on a dual effective action. Finally, we compare our findings with the wall in a "nonminimal" theory with two distinct quark flavors that had been studied previously. In this case the U(1) gauge field trapped on the wall is exactly massless because it is the Goldstone boson of a U(1) symmetry in the bulk spontaneously broken on the wall. The theory on the wall is in the Coulomb phase. We explain why the mechanism of confinement discussed in the first part of the paper does not work in this case, and strings are not formed on the walls.

[1] Unité Mixte de Recherche du CNRS, (UMR 8627).

1 Introduction

Localization of gauge fields on domain walls which are supported by some four-dimensional gauge theories is discussed in the literature for a long time [1, 2, 3, 4, 5, 6]. Elementary domain walls localize U(1) fields. As was explained by Polyakov [7], in 2+1 dimensions the U(1) gauge field is dual to a phase field σ living on S_1. The U(1) gauge theory in 2+1 dimensions can exist in distinct regimes: (i) Coulomb, with the long-range interaction $\ln r$ due to the exchange of the gauge field; (ii) the gauge field is Higgsed, electric charges are screened, interaction due to the exchange of the gauge field falls off exponentially; (iii) the gauge field acquires a mass through the Chern–Simons term, gauge symmetry is unbroken; and (iv) the dual photon field σ gets a mass term. This latter regime is quite peculiar. It might seem that the mass term of the σ field implies short-range interactions. In fact, it is the opposite! Electric charges (seen as the σ field vortices in the dual language) are connected by a flux line which plays the role of a confining string. Interaction between the electric charges grows linearly with the distance r. In terms of σ the string is a domain line very similar to the axion domain walls in 3+1 dimensions. The domain line endpoints are the σ field vortices. (For some reviews see Refs. [8, 9, 10].)

The domain lines of the σ field are the essence of the Polyakov confinement [7]. Polyakov's model is 2+1 dimensional compact electrodynamics. It represents the low-energy limit of SU(2) Yang–Mills theory with one adjoint Higgs field which develops a vacuum expectation value (VEV) breaking SU(2) down to U(1). The mass term for the dual photon is generated by SU(2) three-dimensional instantons (in 2+1 dimensions, technically, they are identical to 't Hooft–Polyakov monopoles [11]). When the U(1) gauge field is dynamically localized on a wall occurring in 3+1 dimensional theory, which of the four regimes listed above is in fact implemented depends on details of the bulk theory.

The first example of a U(1) gauge field localized on a wall, in a fully controllable theoretical setting, was given in [4]. In this example a global U(1) symmetry of the bulk theory, spontaneously broken on the wall, guarantees masslessness of the 2+1 dimensional photon.[2] The U(1) theory on the wall is in the Coulomb regime. When the global U(1) symmetry is explicitly weakly broken in the bulk, the σ field becomes quasi-Goldstone, a σ mass term is

[2]The dual photon σ is the Goldstone field.

generated implying confinement of the electric charges on the wall [5].

In a recent paper [6] a mechanism (developing a concept put forward in [1]) has been suggested that leads to confinement on domain walls. Unlike the models discussed in [4, 5], consideration of Ref. [6] was carried out in non-supersymmetric setting, although the mechanism *per se* is general and can be implemented in a wide class of bulk theories, both supersymmetric or non-supersymmetric. The only requirements to these theories are: they should support both domain walls and Abrikosov–Nielsen–Olesen (ANO) flux tubes [12] and be minimal (in which sense minimal will be explained later). Far away from the wall the charged field condensate responsible for the ANO flux tubes is "large" and squeezes the flux tube from all directions in the perpendicular plane. Now, if we place such tube inside the wall, where the above condensate vanishes with an exponential accuracy, in the first approximation the confining regime gives place to the Coulomb regime on the wall. The flux tube is still squeezed inside the wall in the direction perpendicular to the wall; however, it swells in the directions parallel to the wall.

In the next approximation one should take into account the fact that there is a residual charged field condensate inside the wall. Although it is exponentially small, it still limits the swelling of the flux tube placed inside the wall in the directions parallel to the wall. The thickness of the flux tube in these directions is exponentially large, but finite. If we go to still larger distances along the wall, (magnetic) charges attached to the endpoints of such a tube experience linear confinement.

The above description is phrased in terms of the charged field condensate and magnetic flux tubes. Needless to say, in actuality we keep in mind a dual picture, presented in Fig. 1: the monopole condensation leading to electric flux tubes. In what follows the dualization will be tacitly assumed. Thus, when we speak of matter fields that condense, we will keep in mind that these local fields present an effective description of monopoles, much in the same way as in the Seiberg–Witten construction [13].

The suggestion put forward in [6] is inspirational. At the same time, operational mode of this mechanism remained unclear, as well as its relation to other regimes implementable in the models with the U(1) gauge field localized on the walls. Moreover, particular models considered in [6] suffer from the wall-antiwall instability. With these instabilities, working out quantitative details does not seem possible.

The purpose of the present paper is to address these issues. We focus on investigation of how this mechanism actually works, and what deformations

or modifications lead to deconfinement. We suggest two stable model examples: one at weak coupling and another using the Seiberg–Witten solution [13] at strong coupling. These models are demonstrated to be working examples of confinement on the domain wall. *En route*, we will also clarify some aspect regarding localization of the gauge fields on the domain walls.

To ensure stability of the model it is necessary to require that two vacua in which the matter fields condense are two *distinct* vacua. Let us call them Confining 1 and Confining 2 (Fig. 1).[3] If the monopole mass in the Coulomb phase is m, the condensate in the center of the wall is roughly $ve^{-md/2}$ where d is the wall thickness. If md is large enough, the condensate inside the wall almost vanishes, and the gauge theory exists inside the wall in the (almost) Coulomb regime. Deviations of this almost Coulomb regime from the perfect Coulomb regime determine the thickness of the flux tube in the directions parallel to the wall.

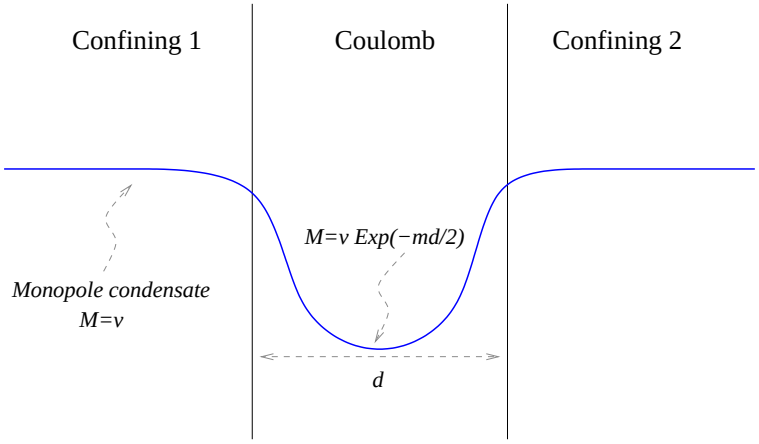

Figure 1: The condensate profile for the wall of the type Confining 1–Coulomb–Confining 2.

The exponentially small deviation from the perfect Coulomb regime inside the wall has a clear-cut interpretation in terms of the field σ. Instead of being the modulus field, as in [4], it becomes a quasimodulus. We work out a method which allows one to calculate its mass directly from the bulk theory. Moreover, introduction of the second matter field, as in [4], can restore the exact modulus status of σ.

[3] In the dual language Confining 1 and Confining 2 read Higgs 1 and Higgs 2.

The paper is organized as follows. In Sect. 2 we discuss some conceptual aspects. Section 3 introduces a "minimal" model, the simplest example which realizes the confinement mechanism discussed by Dvali *et al.* Special attention is given here to discussion of the localization mechanism for the gauge field and formation of the flux tubes in the wall. This example is quasiclassical (the model is weakly coupled) and is phrased in dual terms. The quark field condenses while the monopoles are confined by the Abrikosov–Nielsen–Olesen string. Section 4 provides an example at strong coupling in which condensation that occurs is that of the monopole field. This example is an extension of $\mathcal{N} = 2$ super-Yang–Mills theory (slightly broken to $\mathcal{N} = 1$) considered by Seiberg and Witten. The Seiberg–Witten solution is an essential ingredient which allows us to treat the theory at strong coupling. In Sect. 5 we consider a "nonminimal" theory with two flavors and explain why, in contradistinction with the minimal model of Sect. 2, the gauge field on the wall remain massless despite the presence of a residual condensate in the middle of the wall. The theory on the wall is in the Coulomb regime. The masslessness is backed up by the Goldstone theorem: in the bulk we have an exact global U(1) symmetry which is spontaneously Section 7 summarizes our findings.

2 Conceptual aspects

The basic idea of the gauge field localization suggested in [1] assumes that the bulk four-dimensional theory is in the confining regime while inside the 1+2-dimensional wall we have "less confinement" (or no confinement at all). Then the chromoelectric flux coming from the bulk through a tube spreads out inside the wall. The flux tube-wall junction plays the role of the color source inside the wall. In the dual formulation the bulk theory is Higgsed while inside the wall it is "less Higgsed" (not Higgsed at all in the case of U(1)).

The technical implementation of this idea is not quite straightforward. Indeed, say, in the U(1) case which has just been mentioned the magnetic charges are confined in the bulk. Thus, the magnetic flux from a distant magnetic monopole is squeezed into a tube, and when this tube hits the wall, it spreads out inside the wall. To describe this phenomenon in terms of the standard 1+2-dimensional U(1) gauge theory *on* the wall surface we have to use a duality transformation which converts the magnetic field inside the

wall into a dual electric field of the effective theory on the wall surface. The flux tube-wall junction acts as an *electric* charge source in 1+2-dimensional electrodynamics on the wall. This duality transformation is a crucial element of the construction. The relation between the gauge potential in the bulk and that in the effective low-energy theory on the wall surface is nonlocal.

In 1+2 dimensions the gauge field A_μ is dual to a phase field σ [7]. If a U(1) symmetry is an exact symmetry of the bulk theory, spontaneously broken on the wall, occurrence of the Goldstone field σ localized on the wall is inevitable. Dualizing the above Goldstone field we get massless electrodynamics on the wall. The electric flux from a charge source in the effective theory on the wall surface is spread according to the Coulomb law. If, on the other hand, a global U(1) symmetry is only an approximate symmetry of the bulk theory [5], or even just an approximate symmetry of the domain wall solution [1], we should expect a *pseudo*-Goldstone mode localized on the wall, with a small mass term. With this pseudo-Goldstone mode we get electrodynamics with confinement on the wall, à la Polyakov. The electric flux of the world-volume theory is, in its turn, squeezed on the wall, forming a band of thickness inversely proportional to the pseudo-Goldstone mass. This thickness is exponentially larger than that of the bulk magnetic flux tubes.

These two scenarios are realized in two-flavor and one-flavor models, respectively.

3 The Simplest Example at Weak Coupling

3.1 Theoretical Setting

To introduce the reader to the subject we will start with a toy model that contains all relevant features of the physical phenomenon we want to describe. Consider a U(1) gauge theory with a charged scalar field Q. Our task is to study a domain wall interpolating between Higgs–Coulomb–Higgs vacua. The model is nonsupersymmetric. The simplest choice of the potential seems to be as follows:

$$|Q|^2(|Q|^2 - v^2)^2\,, \tag{1}$$

as suggested in [6]. However, there is a problem with (1), namely the Higgs–Coulomb–Higgs interpolation is a wall-antiwall configuration in this model, which is unstable. Of course, the instability can be made exponentially small, but so are the effects we try to trace.

To create a stable configuration we need at least an extra real neutral field. Consider a system in the Higgs phase, with the U(1) gauge group, a scalar field Q with charge $+1$, and an uncharged scalar a, with the following Lagrangian:

$$L = -\frac{1}{4e^2}(F^{\mu\nu})^2 + \frac{1}{2e^2}(\partial_\mu a)^2 + |\nabla_\mu Q|^2 - V\,, \tag{2}$$

with the potential

$$V = \frac{(a-m)^2(a+m)^2|Q|^2}{m^2} + \frac{e^2}{2}(v^2 - |Q|^2)^2\,. \tag{3}$$

This model is non-renormalizable, but we can still consider it as an effective theory in the infrared.[4] It is obvious then that we have two distinct vacua $a = \pm m$, $|Q| = v$. If we keep $m \gg ev$, there is a large intermediate region inside the domain wall where the VEV of Q is almost zero (see Fig. 2). Even if the theory has no Coulomb vacuum, if we look at the domain wall profile we immediately see that this inside region of the wall is almost in the Coulomb phase. In the limit $m \to \infty$ the wall becomes infinitely thick, and the Higgs VEV in the wall center tends to zero.

To see this we write down the equations of motion for our model. Since we are looking for the domain wall solution we assume that all fields are static and depend only on a single spatial coordinate z (the wall is perpendicular to the z-axis), and drop the gauge field. We have

$$\partial_z^2 a = 4a\,\frac{a^2-m^2}{m^2}\,Q^2\,,$$

$$\partial_z^2 Q - Q\,\frac{(a^2-m^2)^2}{m^2} - e^2(|Q|^2 - v^2)\,Q\; = 0\,. \tag{4}$$

In the leading approximation the quark field Q vanishes inside the wall. Then the first equation above gives for the neutral scalar a

$$a \approx 2m\,\frac{z-z_0}{d}, \tag{5}$$

[4]This example can be embedded in supersymmetric QED (SQED) with the Fayet–Iliopolous D-term, the superpotential

$$W = Q\tilde{Q}\;\frac{(a-m)(a+m)}{m}\,,$$

and in a vacuum with $\tilde{Q} = 0$.

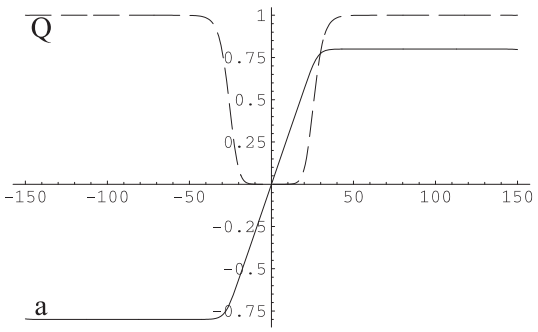

Figure 2: Domain wall in the toy model (2), (3). The profile of the $a(z)$ field is presented by the solid line while that of $Q(z)$ by dashed. The horizontal axis presents the direction z perpendicular to the wall.

where z_0 is the center of the wall, while d is its thickness, to be determined below. In Eq. (5) we take into account the a-field boundary conditions, $a \to \pm m$ at $z \to \pm\infty$. Substituting (5) in the second equation in (4) we can write the following equation for the profile field Q, neglecting the non-linear terms:

$$\partial_z^2 Q = Q \left\{ \frac{16m^2}{d^4} \left[(z - z_0)^2 - \frac{d^2}{4} \right]^2 - e^2 v^2 \right\} . \tag{6}$$

Below we will show that $d \sim m/e^2v^2$. Taking this into account, inside the wall, near its left edge,

$$1/ev \ll z - z_0 + \frac{d}{2} \ll d \,, \tag{7}$$

we can simplify the above equation by dropping the second term in the curly brackets and replacing $z - z_0 - d/2$ by $-d$. Then we get

$$\partial_z^2 Q = Q \, \frac{16m^2}{d^2} \left(z - z_0 + \frac{d}{2} \right)^2 . \tag{8}$$

The solution of this equation obviously has the form

$$Q \approx v \, e^{-\frac{2m}{d}(z - z_0 + \frac{d}{2})^2} , \tag{9}$$

where we use Eq. (7).

Much in the same way, near the right edge of the wall at

$$1/ev \ll -\left(z - z_0 - \frac{d}{2}\right) \ll d \tag{10}$$

we derive from (4)

$$Q \approx v\, e^{-\frac{2m}{d}(z-z_0-\frac{d}{2})^2}\,. \tag{11}$$

Note that these quark profiles are similar to those obtained in [4] in supersymmetric QED with two quark flavors, see Sect. 4.

Let us estimate d in the limit $m \gg ev$. In the inside region the VEV of Q almost vanishes while a is linear in z. In order to estimate the thickness of this region (i.e. the wall thickness), let us first estimate the wall tension as a function of d and then minimize it with respect to d,

$$T_{\rm wall} \sim \frac{e^2 v^4}{2} d + \frac{(2m)^2}{de^2}\,. \tag{12}$$

The assumptions for this estimation are that for $m \gg ev$ the dominating contributions to the energy come from the potential and kinetic terms of the a field. The minimum is achieved at

$$d = \frac{2\sqrt{2}m}{e^2 v^2}\,, \tag{13}$$

where ev is the photon mass in the bulk. The tension of the wall is of the order of

$$T_{\rm wall} \sim 2\sqrt{2}\, m\, v^2. \tag{14}$$

In what follows, we shall be interested in trapping gauge fields, inside this domain wall. Localization of gauge fields on lower-dimensional topological objects is, generally speaking, a nontrivial task. Massless scalars can be localized as Goldstone bosons of continuous symmetries spontaneously broken on the given topological defects. Massless fermions can be localized via Jackiw–Rebbi's and other index theorems [14] (see [15, 16]). We shall discuss this issue in more detail in Section 6.

As discussed in Ref. [4], we can consider the following gauge invariant order parameter:

$$e^{i\sigma} = v^{-2}\bar{Q}(-\infty)e^{i\int A_z dz}Q(+\infty)\,. \tag{15}$$

The difference with the 2-flavor model considered in [4], and discussed in Section 5, is that the two scalar fields at the edges of the Wilson line are now

the same. This implies that we do not have a strictly massless gauge field localized on the wall. This is because the expectation value of the matter field never exactly vanishes inside the wall.

Let us denote the expectation value of the condensate $|Q|$ in the wall center ($z = z_0$) by v_0,

$$v_0 = |Q(z = z_0)| \ . \tag{16}$$

In the limit in which $m \gg ev$, the domain wall is thick and v_0 is very small. A numerical fit in the range $0.3\, v < m < 0.6\, v$ and $0.15 < e < 0.2$ shows that to a very good approximation [5]

$$v_0 \approx v \exp\left(-0.88\, \frac{m^2}{e^2\, v^2}\right) = v \exp\left(-0.31\, d\, m\right) \ . \tag{17}$$

The mass of the gauge field in the bulk is ev; Higgsing inside the wall is exponentially weaker, so that the gauge field mass is $\sim e\, v_0$. To what extent can we speak of localization? The answer depends on the range of the parameters.

Since the domain wall is an object with thickness d a low-energy effective action makes sense only up to energy scales $\sim 1/d$. At higher energies excitations of the wall internal structure become important. Fluctuations of the wall as a whole in the transverse direction (Goldstone modes of the translational symmetry) are massless. They always belong to the low-energy effective action. Other — massive — excitations can be considered a part of the $2 + 1$ dimensional effective action as long as their mass is much smaller than $1/d$. Physics changes in passing from one of the following regimes to another:

$$(i) \qquad 1/d \ll e\, v_0 \ll e\, v \, .$$

In this regime the mass of the gauge field inside the wall is much larger than $1/d$. We can not speak about localization, physics of the wall is essentially four-dimensional.

$$(ii) \qquad e\, v_0 \ll 1/d \ll e\, v \, .$$

[5] This formula, strictly speaking, is valid in the range of parameters indicated above. However, it is likely that it works also for larger d, although it is difficult to check this assumption because accurate numerical calculations are more difficult for larger values of d.

This is the localization limit. Up to energies $\sim 1/d$ the gauge field can be considered as a field localized on the $2+1$ dimensional world volume.

$$(iii) \qquad e\,v_0 \ll e\,v \ll 1/d\,.$$

In this case the gauge field is localized only up to energies $e\,v$. Due to leakage in the bulk no localization occurs at energies from $\sim ev$ to $1/d$.

Focusing on the regimes (ii) and (iii) we ask ourselves whether or not a quasimoduli field lives on the wall in these cases.

3.2 Modulus or quasimodulus on the wall

First, we need to explain why we expect a U(1) quasimodulus on the wall world volume. We begin by presenting the simplest solutions that describe localization of the gauge field: a constant magnetic field and a constant electric field. From now on we will always work in the gauge $A_z = 0$.

A constant magnetic field inside the wall is parallel to the wall surface. Let us assume the magnetic field to be aligned along the x axis, $\vec{B} = B\hat{x}$ where $\hat{x}$ is the unit vector along x. We can construct it in the following way. At negative z we take the field $Q = ve^{iky}$ and the gauge field $A_2 = k$ (or, which is the same, $A_y = -k$. At positive z we take $Q = v$ and $A_y = 0$. In this way in two vacua, to the left and to the right of the wall, the field configuration is pure gauge. Inside the wall, A_y linearly interpolates between $-k$ and 0 on the interval of size d. The magnetic field is $B_x = -\partial_z A_y = k/d$. The magnetic flux per unit length in the y direction is $\int dz B_x = k$. The magnetic field inside the wall is a vector on the wall since it can be oriented either along $\hat{x}$ or along $\hat{y}$.

The electric field inside the wall can only be perpendicular to the wall surface, aligned along $\hat{z}$. Thus, on the wall it must be interpreted as a pseudoscalar. To obtain such an electric field inside the wall consider $Q = ve^{i\omega t}$ at negative z and $A_t = \omega$. At positive z we have $Q = v$ and $A_t = 0$. Inside the wall A_t linearly interpolates between ω and 0. The electric field inside the wall is $E_z = -\partial_z A_t = \omega/d$.

Of course, from the $2+1$ dimensional point of view the picture must be dualized, since in 2+1 dimensions it is the electric field F_{0i} which is a vector while the magnetic field F_{12} is a scalar. For example, $E_x^{(2+1)} = B_x^{(2+1)} =$

$-\partial_z A_x$ and $B^{(2+1)} = B_z^{(2+1)} = -\partial_z A_t$. In other words,

$$F_{\mu\nu}^{(2+1)} = \frac{1}{2}\epsilon^{\mu\nu\rho z} F_{\rho z}\,, \qquad \mu,\nu,\rho = 0,1,2\,. \tag{18}$$

Now we can further dualize $F_{\mu\nu}^{(2+1)}$ à la Polyakov, expressing $F_{\mu\nu}^{(2+1)}$ in terms of a phase fields σ,

$$\frac{1}{2}\epsilon_{\mu\nu\rho} F_{\nu\rho}^{(2+1)} = \frac{1}{d}\partial_\mu \sigma \tag{19}$$

Assembling everything together we have, with our gauge choice

$$B_x^{(3+1)} = -\partial_z A_y \qquad = \qquad E_x^{(2+1)} = \frac{1}{d}\,\partial_y \sigma\,, \tag{20}$$

$$B_y^{(3+1)} = \partial_z A_x \qquad = \qquad E_y^{(2+1)} = -\frac{1}{d}\,\partial_x \sigma\,, \tag{21}$$

$$E_z^{(3+1)} = -\partial_z A_t \qquad = \qquad B^{(2+1)} = \frac{1}{d}\,\partial_t \sigma\,. \tag{22}$$

Note that the angle field σ exactly corresponds to the phase of Q at negative z relative to that at positive z.

We can use unitary gauge which ensures that $Q = v$ in both vacua at $z \to \pm\infty$. In this gauge the constant magnetic field inside the wall looks as follows. The gauge field $A_\mu = 0$ in both vacua, while inside the wall

$$A_z = \frac{1}{d}\,\sigma(x,y), \qquad A_x = A_y = 0. \tag{23}$$

This gauge potential gives the magnetic field strength shown in equations above.

As discussed before, one can consider the gauge invariant order parameter (15). The kinetic term for the gauge field, expressed as a function of the σ modulus, takes the form (cf. [4])

$$\mathcal{L}_{2+1} = \frac{1}{2\, e_{3+1}^2\, d}\ \partial_\mu \sigma \partial_\mu \sigma\,. \tag{24}$$

3.3 Potential for the quasimodulus

As was mentioned, in the model at hand, the phase field σ is not an exact modulus. A potential $V(\sigma)$ is generated forcing $\sigma = 0$ in the true vacuum

which is unique. In the localization limit of large d we can nevertheless speak of a $2+1$ dimensional effective theory for σ, since the σ field mass is much smaller than the excitation energy of the domain wall $\sim 1/d$. In the leading approximation the σ field Lagrangian will be of the sine-Gordon type,

$$\mathcal{L}_{2+1} = \frac{1}{2e^2\, d}\ \partial_\mu\sigma\partial_\mu\sigma - \Delta\cdot\left(\sin\frac{\sigma}{2}\right)^2 \tag{25}$$

where Δ is the difference between two tensions: the tension of the $\sigma = 0$ wall and and that of the $\sigma = \pi$ wall. The mass of σ is

$$m_\sigma \approx \sqrt{\frac{\Delta\, e^2\, d}{2}}\,. \tag{26}$$

Explicit calculations of the quasimodulus potential $V(\sigma)$ are not easy. The minimal tension domain wall corresponds to the lowest energy $\sigma = 0$. Walls with $\sigma \neq 0$ are not static solutions of the equation of motion since they decay. To study such solutions of the equation of motion we have to deal with more than one parameter.

To explain what the last sentence means we consider the solution with a constant magnetic field in the $\hat{y}$ direction (see Fig. 3).

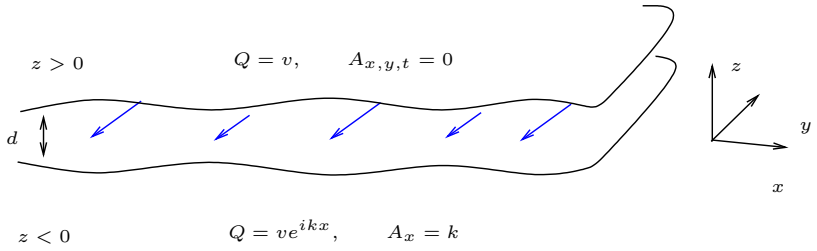

Figure 3: An (almost) constant magnetic field inside the domain wall. From the point of view of the quasi modulus σ it correspond to an "almost" linear solution $\sigma = kx + \ldots$. The dots stand for small modulations. When $\sigma \approx 0$, the wall is thinner and the magnetic field larger. At $\sigma \approx \pi$ the magnetic field is smaller and the wall thicker. The amplitude of the oscillations in $|\vec{B}|$ and thickness depends on the mass of the quasimodulus. In the limit of vanishing mass we recover the constant magnetic field solution.

As a first approximation, we can choose $Q = ve^{ikx}$ and $A_x = k$ at $z < 0$, and $Q = v$ and $A_x = 0$ at $z > 0$, similar to the discussion above. This gives

a constant magnetic field $B_y = k/d$ inside the wall. But it is clear that, due to a nonvanishing (albeit small) Q condensate inside the wall, this is *not* the exact solution. The latter requires modulations of k. One can understand this circumstance both from the bulk and from the brane point of view. The bulk explanation (see Fig. 3) is as follows. Due to topological reasons, the field Q must exactly vanish at some x and $z \approx 0$ each time the relative phase σ rotates by 2π. The lines (in the y direction) on which Q vanishes are the lines where the magnetic field reaches its maximum. We also expect the thickness of the wall to be a little bit larger around these lines.

From the point of view of the $2+1$ dimensional effective action (25) it is also clear that $\sigma(y) = kx$ with k constant is not a solution once the sine term is switched on. The derivative $d\sigma/dx$ will be larger at the top of the potential ($\sigma = \pi$) and smaller at the bottom ($\sigma = 0$).

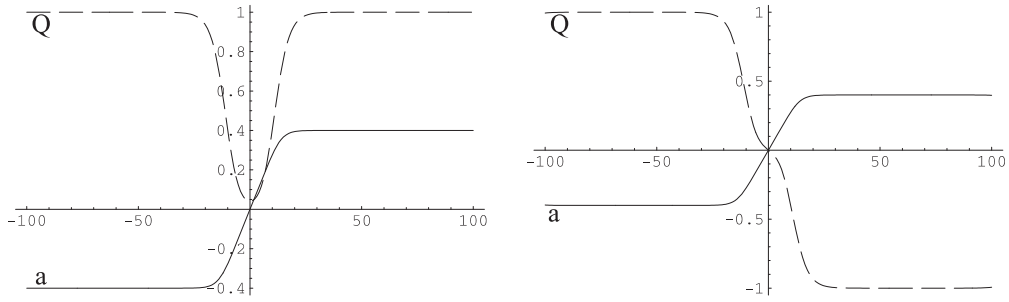

Figure 4: Left: the stable wall ($\sigma = 0$). Right: the unstable wall ($\sigma = \pi$). In this specific example, even though the Higgs VEV is not so small in the middle of the stable wall, there is just a 2% t difference between the tensions of the unstable and stable walls.

There is a trick one can use to detect the quasimodulus. At $\sigma = \pi$ the wall solution corresponds to the maximum of the potential $V(\sigma)$. It is stationary but unstable. In this solution the Q field vanishes exactly in the middle of the wall, at $z = 0$. We can easily get the solution if we impose two conditions: (i) the field Q is real; (ii) Q changes sign in passing from one side of the wall to the other, see Figs. 4 and 5. The difference between the tensions of the unstable and stable walls will determine Δ in Eq. (25).

The mass term for the σ field, is what induces confinement inside the domain wall. In Figure 3 we discussed how a constant magnetic field solution is deformed by the mass term. There are modulations of the thickness of the wall, and magnitude of the magnetic field. These modulations are nothing

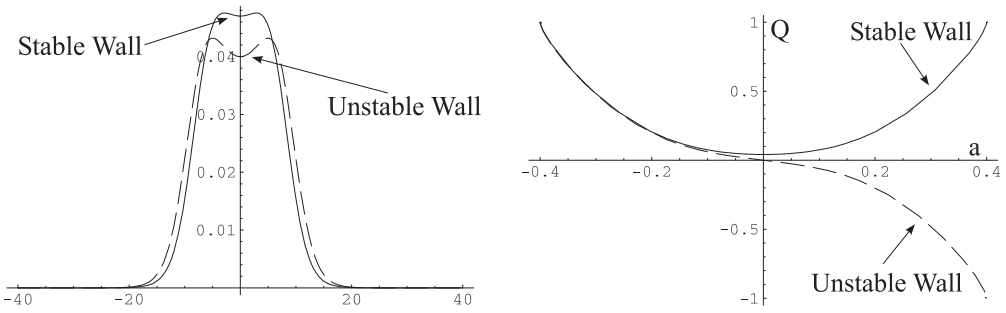

Figure 5: Left: the energy density inside the stable wall (solid line) and the unstable wall (dashed line). In the center of the wall, the unstable wall has a lower energy density. On the other hand, the unstable wall is thicker and this make its total tension larger than that of the stable wall. Right: both domain walls in the (a, Q) plane.

but the flux tubes, all lined together. A single winding in the phase σ, a kink ot the sine-Gordon model (25), is a domain line from the wall point of view. The mass term is what stabilizes the thickness of this kink, that otherwise would spread to ∞. These, from the point of view of the bulk theory, are the confining vortices bounded inside the domain wall.

3.4 A direct estimate of the σ mass term

The Lagrangian of the model under consideration has no exact or approximate global U(1) symmetry. However, the domain wall solution does have such an approximate symmetry. Indeed, let us start from the limit $m/(ev) \to \infty$. In this limit the wall edges become infinitely sharp while the absolute value of the field Q inside the wall vanishes. Then the field configuration under consideration has two U(1) symmetries: $Q(z > z_0 + d/2) \to e^{i\alpha} Q(z > z_0 + d/2)$ and $Q(z < z_0 - d/2) \to e^{i\beta} Q(z < z_0 - d/2)$, with independent phases α and β. The common U(1) symmetry, with $\alpha = \beta$, is gauged. The U(1) phase rotation of $Q(z > z_0 + d/2)$ relative to $Q(z < z_0 - d/2)$ remains as an exact global U(1) symmetry.

If we keep $m/(ev)$ finite, then $Q(z_0)$ does not vanish and, because of continuity of the field Q, the above symmetry becomes approximate. This is due to the fact that now one must continuously evolve the phase of Q from zero at $z = z_0 - d/2$ up to a given σ at $z = z_0 + d/2$. With the z dependent phase inside the wall, the wall configuration no longer presents the exact

solution. The question is how to deal with such a situation.

This is quite similar to the treatment of quasizero modes in the instanton-anti-instanton background field. To deal with them one routinely uses the valley method [17]: in the functional space one finds a direction corresponding to the bottom of the valley and fixes the coordinate along this direction "by hand." In the problem at hand the coordinate to be fixed can be defined as the phase σ in the expression $Q(z = z_0 + d/2) = e^{i\sigma}Q(z = z_0 - d/2)$ (in the $A_z = 0$ gauge). For simplicity we will assume $\sigma(z = z_0 + d/2)$ to be small. Then, given the above boundary condition, minimization of the energy functional gives that inside the wall

$$\sigma(z) \approx \frac{z - z_0 + (\delta/2)}{\delta}\,\sigma\,, \tag{27}$$

where δ is the size of the region inside the wall where phase σ is changing, $\delta < d$. It is a free parameter and we estimate it below by minimization procedure.

As for the ansatz for the scalar field inside the wall we choose the sum of the profile functions (9) and (11) at the left and right edges of the wall. We have

$$Q \approx v\,\left[e^{-\frac{2m}{d}(z-z_0+\frac{d}{2})^2} + e^{-\frac{2m}{d}(z-z_0-\frac{d}{2})^2}\right]\,\exp\left(i\,\frac{z - z_0 + (\delta/2)}{\delta}\,\sigma\right). \tag{28}$$

It is quite obvious that the only extra term in the energy functional (2), (3) comes from $|\partial_z Q|^2$ with the derivative acting on the phase, i.e. $(Q\partial_z\sigma)^2$. Thus, the potential energy associated with $\sigma \neq 0$ (at small σ) is

$$V(\sigma) = \int dz\,\left(Q\frac{\sigma}{\delta}\right)^2 \sim \sigma^2\,\frac{v^2}{\delta^2}\,\int_{-\delta/2}^{\infty} dz\,e^{-\frac{2m}{d}(z+\frac{d}{2})^2} \sim \sigma^2\,\frac{v^2}{\delta^2 ev}\,e^{-\frac{m}{2d}(d-\delta)^2}\,. \tag{29}$$

Minimizing this with respect to δ we get

$$e^2v^2(d-\delta) \sim \frac{1}{\delta}. \tag{30}$$

Assuming that $\delta \ll d$ we have

$$\delta \sim \frac{1}{e^2v^2\,d} \sim \frac{1}{m}, \tag{31}$$

which confirms our assumption, since $\delta/d \sim \frac{e^2v^2}{m^2} \ll 1$.

Substituting δ from (31) to the potential (29) we get

$$V(\sigma) \sim \sigma^2\, v^2\, \frac{m^2}{ev}\, e^{-\frac{md}{2}}, \tag{32}$$

which shows that the potential for σ is exponentially small and is determined by the value of the scalar field in the middle of the wall. Using more accurate numerical estimate (16) for the value v_0 we finally get

$$V(\sigma) \sim \frac{v_0^2\, m^2}{ev}\, \sigma^2\,. \tag{33}$$

This estimate implies, in turn, that

$$\tilde{m}_\sigma \sim ev_0\, \left(\frac{m}{ev}\right)^{3/2}\,. \tag{34}$$

3.5 A numerical check

We have now two different estimations of m_σ. One of them (Eq. (26)) is given in term of Δ, which is the difference in tension between the $\sigma = \pi$ and the $\sigma = 0$ wall. The other one (Eq. (34)) is given in terms of the residual condensate v_0 at the center of the domain wall. It is interesting to compare them for a cross check.

		m				
		0.30	0.35	0.40	0.45	0.50
e	0.2	2.5×10^{-2}	6.0×10^{-3}	1.1×10^{-3}	1.6×10^{-4}	1.8×10^{-5}
	0.19	1.6×10^{-2}	3.2×10^{-3}	4.8×10^{-4}	5.7×10^{-5}	5.1×10^{-6}
	0.18	9.0×10^{-3}	1.5×10^{-3}	1.8×10^{-4}	1.7×10^{-5}	1.1×10^{-6}
	0.17	4.7×10^{-3}	6.2×10^{-4}	5.8×10^{-5}	3.9×10^{-6}	1.9×10^{-7}
	0.16	2.1×10^{-3}	2.1×10^{-4}	1.5×10^{-5}	7.0×10^{-7}	2.2×10^{-8}

Table 1: Values of Δ for $v = 1$ and different values of (m, e).

In Table 1 numerical results for Δ are shown for some values of the parameters. In Table 2 the corresponding values of v_0 are presented. We can then use these values for a comparison the two independent estimations m_σ, $\tilde{m}_\sigma$. The results are shown in Table 3. The proximity of the ratio $m_\sigma/\tilde{m}_\sigma$ to unity is obvious. The agreement is indeed quite good. We can also verify that the localization condition $e\, v_0 \ll 1/d$ is satisfied very well for $m \geq 0.4\, v$ and $e < 0.2$.

		m				
		0.30	0.35	0.40	0.45	0.50
e	0.2	2.6×10^{-1}	1.1×10^{-1}	4.1×10^{-2}	1.4×10^{-2}	4.5×10^{-3}
	0.19	2.0×10^{-1}	7.7×10^{-2}	2.7×10^{-2}	8.4×10^{-3}	2.3×10^{-3}
	0.18	1.5×10^{-1}	5.2×10^{-2}	1.6×10^{-2}	4.5×10^{-3}	1.1×10^{-3}
	0.17	1.0×10^{-1}	3.2×10^{-2}	9.0×10^{-3}	2.2×10^{-3}	4.5×10^{-4}
	0.16	6.8×10^{-2}	1.9×10^{-2}	4.5×10^{-3}	9.1×10^{-4}	1.5×10^{-4}

Table 2: Values of v_0 for $v = 1$ and different values of (m, e).

		m				
		0.30	0.35	0.40	0.45	0.50
e	0.2	1.08	1.08	1.08	1.05	1.01
	0.19	1.07	1.08	1.07	1.03	0.99
	0.18	1.08	1.08	1.05	1.01	0.97
	0.17	1.08	1.07	1.03	0.99	0.95
	0.16	1.08	1.06	1.01	0.97	0.92

Table 3: Values of $m_\sigma/\tilde{m}_\sigma$ for $v = 1$ and different values of (m, e). m_σ is given in Eq. (26) and $\tilde{m}_\sigma$ given by Eq. (34).

4 A Modified Seiberg–Witten framework

4.1 Theoretical Setting

We now turn to a strong coupling example of the confinement phenomenon inside domain walls. The model we will dwell on below is a rather straightforward modification of the Seiberg–Witten (SW) model [13], which supports both domain walls and strings.

The theory of interest is $\mathcal{N} = 2$ gauge theory, with the gauge group $\mathrm{U}(2) = \mathrm{SU}(2) \times \mathrm{U}(1)/Z_2$, with no matter hypermultiplets. The following superpotential which breaks the extended supersymmetry down to $\mathcal{N} = 1$ is then added:

$$W = \alpha \,\mathrm{Tr}\left(\frac{\Phi^3}{3} - \xi\Phi\right). \tag{35}$$

Classically, we have three vacua, with ϕ equal to

$$\begin{pmatrix} \sqrt{\xi} & 0 \\ 0 & \sqrt{\xi} \end{pmatrix}, \qquad \begin{pmatrix} \sqrt{\xi} & 0 \\ 0 & -\sqrt{\xi} \end{pmatrix}, \qquad \begin{pmatrix} -\sqrt{\xi} & 0 \\ 0 & -\sqrt{\xi} \end{pmatrix}. \tag{36}$$

The first and the last vacua preserve the non-Abelian SU(2) gauge symmetry. Strong coupling effects à la Seiberg and Witten will then split each of them into two vacua (the monopole and dyon vacua). The vacuum in the middle preserves only the U(1) × U(1) gauge symmetry, and is not split. We, thus, expect in total five vacua, for generic values of ξ.

If we set α at zero, the U(1) and SU(2) sectors get completely decoupled. Since there are no matter hypermultiplets, only a nonvanishing superpotential can make the two sectors communicate with each other. Dynamics of the U(1) sector is trivial, while the SU(2) sector is described by the Seiberg–Witten solution [13]. We parametrize the moduli space by

$$\Phi = \begin{pmatrix} a_0 + a_3 & 0 \\ 0 & a_0 - a_3 \end{pmatrix}. \tag{37}$$

The conventional SW solution is written in terms of the invariant

$$u = 2a_3^2 \,. \tag{38}$$

In our case

$$\mathrm{Tr}\,\Phi = 2a_0, \qquad \mathrm{Tr}\,\Phi^2 = 2a_0^2 + 2a_3^2, \qquad \mathrm{Tr}\,\Phi^3 = 2a_0^3 + 6a_3^2 a_0 \,, \tag{39}$$

and there is an invariant way to parameterize the moduli space [18, 19] by

$$u_1 = \mathrm{Tr}\,\Phi \,, \qquad u_2 = \frac{1}{2}\mathrm{Tr}\,\Phi^2 \,. \tag{40}$$

The trace of of Φ^3 can be expressed in terms of $u_{1,2}$,

$$\mathrm{Tr}\,\Phi^3 = \frac{3}{2}(\mathrm{Tr}\,\Phi)(\mathrm{Tr}\,\Phi^2) - \frac{1}{2}(\mathrm{Tr}\,\Phi)^3 \,. \tag{41}$$

This relation is not modified by quantum corrections.

After the superpotential (35) is switched on, the moduli space is lifted. Five discrete vacua described above survive. This is a special case of the set-up considered in Refs. [18, 19]. The positions of the vacua are the following

(see Appendix 7 for more details). The value of u_2 is ξ for all five vacua. It is not modified by quantum corrections. The Coulomb vacuum in the middle is not modified by quantum correction either. It lies at

$$u_1 = 0\,, \quad u_2 = \xi\,. \tag{42}$$

The monopole-1 and dyon-1 vacua $\phi = \mathrm{diag}\,(\xi, \xi)$ are at

$$u_1 = 2\sqrt{\xi - \Lambda^2},\ \ u_2 = \xi \quad \text{and} \quad u_1 = 2\sqrt{\xi + \Lambda^2},\ \ u_2 = \xi\,, \tag{43}$$

respectively. The dyon-2 and monopole-2 vacua from $\phi = \mathrm{diag}\,(-\xi, -\xi)$ are at

$$u_1 = -2\sqrt{\xi - \Lambda^2},\ \ u_2 = \xi \quad \text{and} \quad u_1 = -2\sqrt{\xi + \Lambda^2},\ \ u_2 = \xi\,. \tag{44}$$

In the limit $\sqrt{\xi} \gg \Lambda$ the Coulomb vacuum is such that the electric coupling

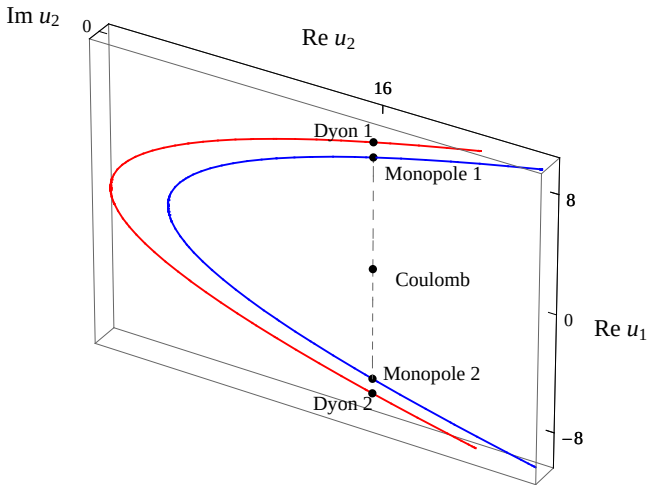

Figure 6: Five vacua of the model in the limit $\sqrt{\xi} \gg \Lambda$. (In the plot we set $\Lambda = 1$, $\xi = 4$). The dashed line connects the monopole-1, Coulomb, and monopole-2 vacua. This is the composite domain wall we will analyze in what follows. Note that all five vacua are aligned.

is small,

$$e_3^2 = \frac{1}{\ln\left(\sqrt{\xi}/\Lambda\right)}\,. \tag{45}$$

The five vacua in this limit are depicted in Fig. 6.

As ξ decreases and becomes of order Λ, the Coulomb vacuum enters a strong coupling regime. At the critical value $\xi = \Lambda^2$ the Coulomb vacuum lies exactly in the monopole singularity and coalesces with two monopole vacua. Around this critical value, the Coulomb vacuum is such that the magnetic coupling is small, so we can use the same set of low-energy effective variables to describe both the Coulomb and the confining vacua. In this section we will study (in the limit $|\xi - \Lambda^2| \ll \Lambda^2$) the domain walls connecting the Coulomb and the confining vacua. It is convenient to introduce a dimensionless parameter

$$\epsilon^2 = \frac{\xi - \Lambda^2}{\Lambda^2} \,. \tag{46}$$

We will work in the limit $|\epsilon| \ll 1$, but keeping three vacua separate (i.e. $\epsilon \neq 0$).

The effect of the superpotential W in the infrared theory, near the monopole vacuum, is described by the following effective superpotential:

$$\tilde{W} = \frac{A_{3D} M \tilde{M}}{\sqrt{2}} + \frac{\alpha(2A_0^3 + 6u(A_{3D})A_0)}{3} - 2\alpha\xi A_0 \,, \tag{47}$$

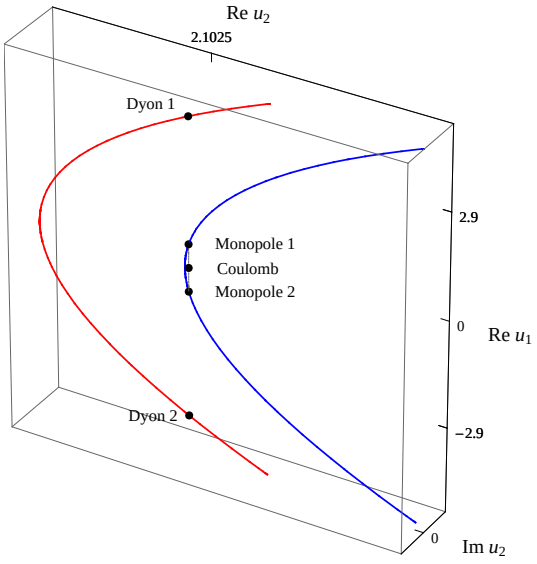

Figure 7: As ξ becomes smaller, we reach a critical point where the Coulomb vacua lies exactly on the monopole singularity. Around this point we can use the magnetic effective action to describe the wall. It remains weakly coupled in all three vacua of interest ($\Lambda = 1$, $\xi = 1.45$ in this plot).

where we can use

$$u(A_{3D}) \approx \Lambda^2 - 2i\Lambda A_{3D} - \frac{1}{4}A_{3D}^2 + \dots \,. \tag{48}$$

The F-term part of the scalar potential is

$$V_F = e_{3D}^2 |\frac{M\tilde{M}}{\sqrt{2}} + 2\alpha u' A_0|^2 + 4e_0^2\alpha^2 |A_0^2 + u - \xi|^2 + \frac{|MA_{3D}|^2 + |\tilde{M}A_{3D}|^2}{2}\,, \tag{49}$$

while the D-term part is

$$V_D = \frac{e_{3D}^2}{2}(MM^\dagger - \tilde{M}\tilde{M}^\dagger)^2\,, \tag{50}$$

where M, $\tilde{M}$ are the monopole superfields. The vacuum expectation values in the confining vacua are (in the limit $\epsilon \ll 1$)

$$A_{3D} = 0, \qquad A_0 = \pm\Lambda\epsilon, \qquad M\tilde{M} = \pm 4\sqrt{2}\, i\, \Lambda^2\alpha\epsilon\,. \tag{51}$$

The dual description is valid in these vacua provided that the monopole condensate is $\ll \Lambda^2$ implying $|\alpha\epsilon| \ll 1$.

The Coulomb vacuum is defined by the following constraints:

$$M = \tilde{M} = 0\,, \qquad A_0 = 0\,, \qquad u(A_{3D}) = \xi\,. \tag{52}$$

The VEV of A_{3D} in the limit $\epsilon \ll 1$ is

$$A_{3D} = \frac{\epsilon^2\Lambda i}{2}\,. \tag{53}$$

A nice feature of the limit $\epsilon \ll 1$ is that we can use the same weakly coupled effective description in all three vacua of interest (Coulomb, monopole-1 and monopole-2). This unified description is also valid for the domain wall interpolating between them. In this sense the situation drastically differs from the case considered in Ref. [20], where no unified description was possible for the domain wall interpolating between the monopole and the dyon vacua considered in [20].

The kinetic terms are

$$\begin{aligned} \mathcal{L}_{\rm kin} &= \frac{1}{4e_{3D}^2}\,(F_{3D}^{\mu\nu})^2 + \frac{1}{4e_0^2}\,(F_0^{\mu\nu})^2 \\ &+ \frac{1}{2e_{3D}^2}(\partial_\mu a_{3D})^2 + \frac{1}{2e_0^2}(\partial_\mu a_0)^2 + |\nabla_\mu M|^2 + |\nabla_\mu \tilde{M}|^2\,. \end{aligned} \tag{54}$$

In the confining vacua the value of the coupling e_{3D} is determined by the monopole condensate,

$$e_{3D}^2 = \frac{1}{\ln\left(\Lambda/\sqrt{|M\tilde{M}|}\right)} \approx \frac{1}{\ln\left(1/\sqrt{|\alpha\epsilon|}\right)}\,. \tag{55}$$

In the Coulomb vacuum the expression for e_{3D}^2 can be found from the Seiberg–Witten expression for $\tau = \theta/(2\pi) + 4\pi i/g^2$,

$$e_{3D}^2 \approx \frac{1}{\ln\left(1/|\epsilon|\right)}\,. \tag{56}$$

An effective coupling $e_{3D}(z)$ along the domain wall profile is a function of the field condensates inside the wall. It interpolates between the two values above, (55) and (56). If we choose $\alpha \sim \epsilon$, then e_{3D}^2 is approximately constant.

Replacing the leading terms in $u(A_{3D})$ in the scalar potential, we get

$$\begin{aligned} V &= e_{3D}^2 \left| \frac{M\tilde{M}}{\sqrt{2}} - 4i\alpha\Lambda A_0 \right|^2 + 4e_0^2\alpha^2 \left| A_0^2 - 2i\Lambda A_{3D} + \Lambda^2 - \xi \right|^2 \\ &+ \frac{|MA_{3D}|^2 + |\tilde{M}A_{3D}|^2}{2} + \frac{e_{3D}^2}{2}(MM^\dagger - \tilde{M}\tilde{M}^\dagger)^2\,. \end{aligned} \tag{57}$$

4.2 Elementary and composite walls

We look for the wall solution in the ansatz:

$$|\tilde{M}| = |M|\,, \tag{58}$$

which automatically guarantees vanishing of the D term. We will assume the phases of $\tilde{M}$ and M to be constant constant in our wall solution. This assumption is to be checked *a posteriori*. Once the phases are constant, they can be chosen at will by virtue of a global gauge rotation. It is convenient to choose

$$\tilde{M} = iM\,. \tag{59}$$

The value of the superpotential in the two confining vacua, monopole-1 and monopole-2, is

$$W = \pm\,\frac{4}{3}\,\Lambda^3\,\alpha\epsilon^3\,. \tag{60}$$

In the Coulomb vacuum the superpotential vanishes. Hence, the tension of the BPS wall interpolating between monopole-1 and monopole-2 vacua, if it existed, would be twice the tension of the BPS wall interpolating between the Coulomb and confining vacua. The latter walls will be referred to as elementary. The former wall can be called composite.

For the elementary wall, we can take M and A_0 real and A_{3D} pure imaginary. Then we can write the following BPS equations: [6]

$$\frac{\partial M}{\partial z} - i\frac{M\, A_{3D}}{\sqrt{2}} = 0\,,$$

$$\frac{\partial A_0}{\partial z} - 2\alpha e_0^2(A_0^2 - 2i\Lambda A_{3D} - \xi + \Lambda^2) = 0\,,$$

$$\frac{\partial A_{3D}}{\partial z} + ie_{3D}^2\left(\frac{M^2}{\sqrt{2}} - 4\alpha\Lambda A_0\right) = 0\,. \qquad (61)$$

The profile functions for the elementary wall interpolating between the confining and the Coulomb vacua, are shown if Fig. 8. In this theoretical set-up,

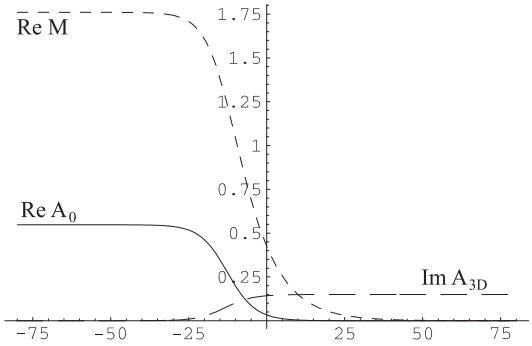

Figure 8: Elementary wall at $\mu = 0$ (see Eq. (62)), A_0 (solid), A_3 (long dashes) and M (short dashes).

no BPS wall interpolating between two confining vacua, monopole-1 and monopole-2, exists. In other words, a composite wall built of two elementary walls at a finite distance from each other, does not exist. Supersymmetric

[6] Note that e_{3D} is a function of the fields $M\tilde{M}$, a_{3D}; this does not change the form of the BPS equations. Our choice $\alpha \approx \epsilon$ guarantees constancy of e_{3D} to a very good approximation. For simplicity, in the numerical calculations we keep e_{3D} constant.

solutions correspond to viscous flows in the first-order equations, starting from monopole-1, following the profile $\tilde{W}$ and ending in monopole-2. It is not difficult to see that such flow cannot be realized in the case at hand. A field configuration interpolating between monopole-1 and monopole-2 is always time-dependent; it represents two elementary walls moving under the influence of a repulsive force between them (see Ref. [21] for a discussion in supersymmetric sigma models). This force falls off exponentially with the wall separation.

4.3 Composite wall stabilization

In order to avoid the problem discussed in Sect. 4.2 and stabilize the composite domain wall, an extra term is introduced in the superpotential,

$$W = \alpha \left(\mathrm{Tr} \left(\frac{\Phi^3}{3} - \xi \Phi \right) + \frac{i\mu}{2} (\mathrm{Tr}\, \Phi)^2 \right), \tag{62}$$

where ξ is chosen as a real parameter, with $\xi > \Lambda^2$, and μ is a real mass parameter, $\mu < \epsilon\, \Lambda$.

In the effective low-energy superpotential we get

$$\tilde{W} = \frac{A_{3D} M \tilde{M}}{\sqrt{2}} + \frac{\alpha(2A_0^3 + 6u(A_{3D})A_0)}{3} - 2\alpha\xi A_0 + 2i\alpha\mu A_0^2 \,, \tag{63}$$

Then, the F term takes the form

$$\begin{aligned} V_F &= e_{3D}^2 \left| \frac{M\tilde{M}}{\sqrt{2}} + 2\alpha u' A_0 \right|^2 + 4e_0^2\alpha^2 \left| A_0^2 + 2i\mu A_0 + u - \xi \right|^2 \\ &+ \frac{|MA_{3D}|^2\, |\tilde{M}A_{3D}|^2}{2} \,. \end{aligned} \tag{64}$$

The Coulomb vacuum remains intact when $\mu \neq 0$ is switched on, and so is the value of the superpotential in the Coulomb vacuum. Both confining vacua have $A_{3D} = 0$. The values of A_0 and the monopole field condensate are

$$A_0 = -\mu i \pm \sqrt{\xi - \Lambda^2 - \mu^2}, \quad M\tilde{M} = i4\sqrt{2}\alpha\Lambda \left(-i\mu \pm \sqrt{\xi - \Lambda^2 - \mu^2} \right) . \tag{65}$$

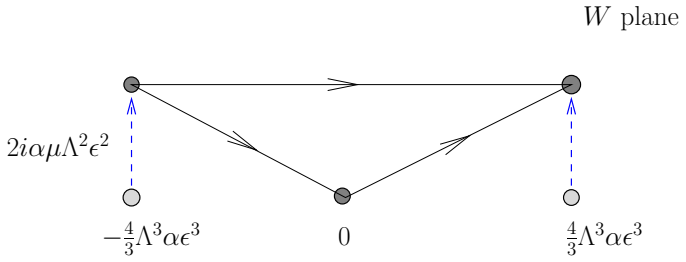

Figure 9: Superpotential values in three vacua, at nonvanishing μ (in the complex $\tilde{W}$ plane).

The values of the superpotential in both confining vacua change (see Fig. 9), being shifted upwards in the complex plane,

$$\tilde{W}_{1,2} = \frac{2}{3}\alpha\left[-2i\mu^3 + 3i(\xi-\Lambda^2)\mu \mp 2(\xi-\Lambda^2-\mu^2)^{3/2}\right]. \tag{66}$$

The tension of the BPS domain wall is given by the absolute value of the difference of the superpotentials at two vacua between which the given wall interpolates. For this reason, if the composite BPS walls exist at $\mu \neq 0$, the composite wall will be stable, see Fig. 9.

In order to write the BPS equations for the elementary wall, we need complex profile functions for each field, M, A_{3D} and A_0. The ansatz $\tilde{M} = iM$ can still be used. Let us introduce a phase (see Ref. [22] for a detailed discussion)

$$\omega = \mathrm{Arg}\,\frac{3\,(\xi-\Lambda^2)\,\mu - 2\mu^3}{2\,(\xi-\Lambda^2-\mu^2)^{3/2}}\,. \tag{67}$$

The BPS equations generalizing those in Eq. (61) to the case $\mu \neq 0$ are

$$\begin{aligned}
&\frac{\partial M^\dagger}{\partial z} - ie^{i\omega}\frac{M\,A_{3D}}{\sqrt{2}} = 0\,,\\
&\frac{\partial A_0^\dagger}{\partial z} - e^{i\omega}2\alpha e_0^2(A_0^2 - 2i\Lambda A_{3D} + 2i\mu\Lambda A_0 - \xi + \Lambda^2) = 0\,,\\
&\frac{\partial A_{3D}^\dagger}{\partial z} + ie^{i\omega}e_{3D}^2\left(\frac{M^2}{\sqrt{2}} - 4\alpha\Lambda A_0\right) = 0\,.
\end{aligned} \tag{68}$$

Numerical solution for the profile functions of the elementary walls at $\mu \neq 0$ is displayed in Fig. 10. For the composite wall we again can use the ansatz

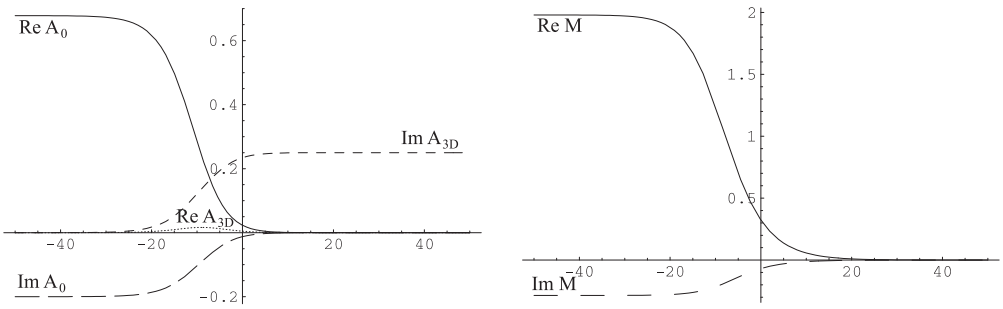

Figure 10: Elementary wall profile functions at nonvanishing μ. Left: $\mathrm{Re}\, A_0$ (solid), $\mathrm{Im}\, A_0$ (long dashes), $\mathrm{Im}\, A_3$ (short dashes), $\mathrm{Re}\, A_3$ (dots). Right: $\mathrm{Re}\, M$ (solid) and $\mathrm{Im}\, M$ (dashed).

$\tilde{M} = iM$. The BPS equations are very similar to the ones for the elementary walls. The only difference is that for the composite wall $\omega = 0$ and the profiles of $\mathrm{Im}\, A_0$ and $\mathrm{Re}\, A_{3D}$ are constant,

$$\mathrm{Im}\, A_0 = -\mu\,, \qquad \mathrm{Re}\, A_{3D} = 0\,. \tag{69}$$

The BPS equations for the non-constant profile functions are

$$\begin{aligned}
\frac{\partial(\mathrm{Re}\, M)}{\partial z} &= -\frac{(\mathrm{Re}\, M)\,(\mathrm{Im} A_{3D})}{\sqrt{2}}\,,\\
\frac{\partial(\mathrm{Im}\, M)}{\partial z} &= \frac{(\mathrm{Im}\, M)\,(\mathrm{Im} A_{3D})}{\sqrt{2}}\,,\\
\frac{\partial(\mathrm{Re}\, A_0)}{\partial z} &= 2\alpha e_0^2((\mathrm{Re}\, A_0)^2 + 2(\mathrm{Im}\, A_{3D})\Lambda - \epsilon^2\Lambda^2 + \mu^2)\,,\\
\frac{\partial(\mathrm{Im}\, A_{3D})}{\partial z} &= -e_3^2\left(\frac{(\mathrm{Re}\, M)^2 - (\mathrm{Im}\, M)^2}{\sqrt{2}} - 4\alpha\Lambda(\mathrm{Re}\, A_0)\right)\,.
\end{aligned} \tag{70}$$

From these equations we deduce that the following quantity remains constant (z-independent):

$$(\mathrm{Re}\, M)(\,\mathrm{Im}\, M) = -2^{3/2}\alpha\mu\Lambda\,. \tag{71}$$

The corresponding profiles are shown in Fig. 11. The boundary conditions are such that $M(\infty) = -iM(-\infty)$. Note that if we try to use the boundary conditions $M(\infty) = iM(-\infty)$, we get an unstable wall, whose tension is

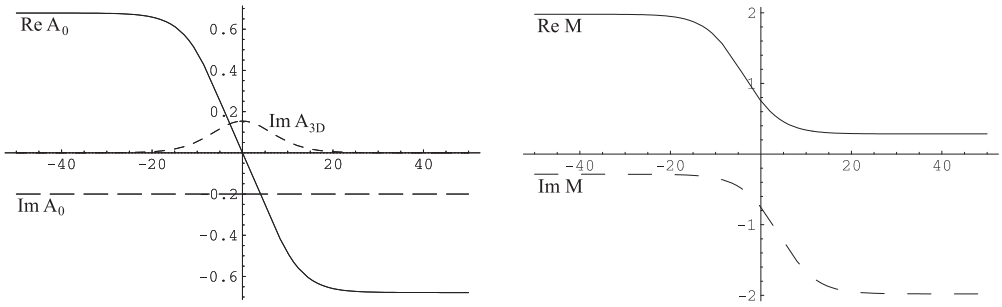

Figure 11: The profile functions of the stable composite wall profiles at nonvanishing μ Left: $\mathrm{Re}\, A_0$ (solid), $\mathrm{Im}\, A_0$ (long dashes), $\mathrm{Im}\, A_3$ (short dashes). Right: $\mathrm{Re}\, M$ (solid) and $\mathrm{Im}\, M$ (dashed).

larger than twice the tension of the elementary wall. The tensions of the BPS walls are given by the central charges,

$$\begin{aligned} T_{12} &= T_{23} = \frac{4\alpha}{3}\sqrt{4(\epsilon^2\Lambda^2-\mu^2)^3+(3\mu\epsilon^2\Lambda^2-2\mu^3)^2}\,, \\ T_{13} &= \frac{16\alpha}{3}(\epsilon^2\Lambda^2-\mu^2)^{3/2}\,, \end{aligned} \tag{72}$$

implying that the composite wall is stable. Note also that the parameter ω is different for the composite and elementary walls. Two out of four supercharges will annihilate each domain wall; but they will be different for the composite and elementary walls.

On symmetry grounds one can state that the real and imaginary parts of the M condensate in the wall center (i.e. at the point $z = 0$) are equal in absolute value. Using the fact that $(\mathrm{Re}\, M(z))(\,\mathrm{Im}\, M(z))$ is constant, it is straightforward to analytically calculate the monopole condensate at the center of the composite domain wall. The expression for the condensate in the wall center is very concise,

$$|\mathrm{Re}\, M(z=0)| = |\mathrm{Im}\, M(z=0)| \approx 2^{3/4}\sqrt{\mu\alpha\Lambda}\,. \tag{73}$$

In the limit $\mu \ll \epsilon\Lambda$ the condensate outside the wall is

$$|\mathrm{Re}\, M(z=\pm\infty)| \approx 2^{5/4}\Lambda\sqrt{\alpha\epsilon}\,, \quad |\mathrm{Im}\, M(z=\pm\infty)| \approx 2^{1/4}\mu\sqrt{\frac{\alpha}{\epsilon}}\,. \tag{74}$$

The ratio of the absolute values of the monopole condensates inside and outside the wall is proportional to $\sqrt{\mu/(\epsilon\Lambda)}$.

4.4 Confinement on the composite domain wall

As in the toy model discussed in Sect. 3, we would like to understand the localization of the (massive) gauge field on the wall as a quasimodulus σ localized on the wall world volume. Previous consideration suggests us to look for an opposite direction rotation of the U(1) phase of the monopole field at $z < 0$ and $z > 0$, respectively. Our target is an exited domain wall (corresponding to $\sigma = \pi$) in which the charged field profile vanishes in the center of the wall (see Fig. 4 pertinent to the toy model of Sect. 3). There is an important difference between the toy model and that of Sect. 4. In the former case the Coulomb phase was not a true vacuum of the theory, while in the latter it is. This implies that imposing the condition $\sigma = \pi$ we get, in fact, two elementary walls, with no binding energy, separated by infinite distance. Needless to say, the condition that typical energies in the low-energy theory must be $\ll 1/d$ cannot be met then. In this formulation it makes no sense to speak of localization and reduction to $2 + 1$ dimensions.

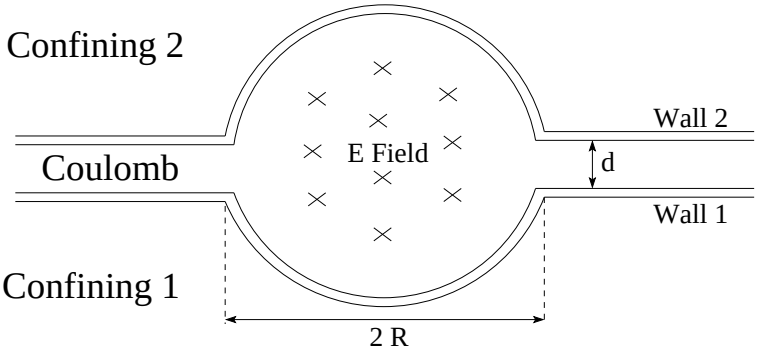

Figure 12: A sketch of an electric flux tube trapped in the middle of the composite wall.

To discuss confinement and localization on the composite wall we must change the setting. Consider the field configuration shown in Fig. 12, which displays a flux tube trapped in the middle of the composite wall. Let us call R the radius of the region where the electric field is localized.

The two-component wall is stabilized at a distance d_0 between the elementary walls. To separate them will cost a finite amount of energy per unit surface of the wall, to be referred to as $\delta T_{\rm w}$. In the model discussed in this section, at the first nonvanishing order in μ, we have

$$\delta T_{\rm w} = 6\,\alpha\,\epsilon\,\Lambda\,\mu^2\,. \tag{75}$$

Denote the electric flux of the vortex by f. An estimate for the tension of the flux tube is

$$T_{\rm ft} \approx \frac{1}{2e_{3D}^2}\,\frac{f^2}{\pi R^2} + 2R\,\delta T_{\rm w}\,. \tag{76}$$

Minimizing with respect to R we arrive at

$$R_* = \left(\frac{f^2}{2\pi\, e_{3D}^2\,\delta T_w}\right)^{1/3}\,. \tag{77}$$

This shows that R_* is a finite quantity, and the flux is indeed squeezed into flux tubes inside the composite domain wall. This is, of course, applicable provided that $\delta T_{\rm w}$ is positive (i.e. the force between two elementary domain walls is attractive, which is the case in the model at hand).

Now, let us consider the case of a constant electric flux per unit length of the wall in the perpendicular direction (analogous to the picture in Fig. 3) We will denote this quantity — flux per unit length — by the same letter f. This flux is trapped in the middle Coulomb vacuum. As a consequence, there is a repulsive contribution to the potential between the two components of the composite wall,

$$T_{\rm wf} = \frac{1}{e_{3D}^2}\,\frac{f^2}{d}\,. \tag{78}$$

In order to find the minimum of the overall potential, we have to add this to the domain wall tension $T_{\rm w}$ considered as a function of d. At large distance $T_{\rm w}$ has just an exponential tail in d; therefore, the-long range force is repulsive, as follows from Eq. (78). If the flux f is small, however, the global minimum of the inter-wall potential is still at finite d. There is a critical value of f — let us call it f_0 — for which the elementary domain walls at the equilibrium will be separated by a infinite distance. A simple energy estimate can be used to evaluate the value of f_0,

$$\frac{1}{e_{3D}^2}\,\frac{f_0^2}{d_0} > \delta T_{\rm w}\,, \quad f_0 = e_{3D}\sqrt{d_0\,\delta T_{\rm w}}\,, \tag{79}$$

where d_0 is the domain wall separation at zero f.

Thus, although the low-energy description in the Seiberg–Witten motivated model at hand is not of the sine-Gordon type (cf. (25)), the quasimodulus-based low-energy description is still valid at $|\sigma| \ll \pi$: a mass term $m\sigma^2$ is generated.

5 Two-Flavor Model

5.1 $\mathcal{N} = 2$ SQED with two flavors

At this point one is tempted to say that the fact that the gauge field localized on the wall weakly confines is due to residual exponentially small VEV's of the Higgs field inside the wall. In this case, the absence of the Coulomb regime on the wall would be a universal phenomenon. In fact, we know that this is not the case [4] (see also the review paper [8]). In Ref. [4] $\mathcal{N} = 2$ SQED with two flavors was considered. This model has a domain wall with a phase field σ localized on it. This field is a Goldstone of a spontaneously broken U(1) and, thus, remains exactly massless. Upon Polyakov's dualization it represents a U(1) gauge field on the wall in the Coulomb regime. Moreover, in the same paper [4] it was shown that a magnetic flux tube coming from the bulk in the perpendicular to the wall direction ends on the wall creating a vortex of the σ field. Upon Polyakov's dualization this vortex is interpreted as an electric charge, a source of the electric field on the wall. Two such sources interact through the Coulomb potential at large distances (logarithmic in 2+1 dimensions).

Residual exponentially small VEV's of the Higgs field inside the wall are certainly important. For instance, in the toy model considered in Sect. 3 the σ field turns out to be a quasimodulus only because the wall at hand is very thick implying exponential suppression of the Higgs field inside the wall. If the wall was thin, σ would be heavy, and the only light field on its world volume would be the translational modulus. In the two-flavor model we can introduce σ as a relative phase between q_1 on one side of the wall and q_2 on the other side. Because these fields are different, there is no need in a z dependent interpolation of σ inside the wall, as was the case in the one-flavor model. This is the technical reason for its masslessness.

Below we will illustrate the emergence of the *exact* moduli field σ in $\mathcal{N} = 2$ SQED with 2 flavors analyzing it in a regime somewhat different from that of Ref. [4]. This moduli field remains massless even in the limit of thin wall. Thus, the mode of implementation of 2+1 dimensional electrodynamics on the wall world volume — Coulomb vs. confinement — is a dynamical issue.

Consider $\mathcal{N} = 2$ SQED with two flavors and the matter mass terms chosen as follows:

$$m_1 = m\,, \qquad m_2 = -m\,, \quad \Delta m \equiv m_1 - m_2 \equiv 2m\,. \tag{80}$$

We will introduce the Fayet–Iliopoulos term ξ through the superpotential. Then the bosonic part of the action can be written as

$$S = \int d^4x \left\{ \frac{1}{4e^2} F_{\mu\nu}^2 + \frac{1}{e^2} |\partial_\mu a|^2 + \bar{\nabla}_\mu \bar{q}_A \nabla_\mu q^A + \bar{\nabla}_\mu \tilde{q}_A \nabla_\mu \bar{\tilde{q}}^A + V_D + V_F \right\}, \tag{81}$$

where the scalar potential is the sum of D and F terms,

$$\begin{aligned} V_D &= \frac{e^2}{8} \left(|q^B|^2 - |\tilde{q}_B|^2 \right)^2 , \\ V_F &= \frac{1}{2} \left| q^B (a + \sqrt{2} m_B) \right|^2 + \frac{1}{2} \left| \tilde{q}_B (a + \sqrt{2} m_B) \right|^2 \\ &+ \frac{e^2}{2} \left| \tilde{q}_A q^A - \frac{\xi}{2} \right|^2 . \end{aligned} \tag{82}$$

This theory has two vacua, and a domain wall interpolating between them. It was fully analyzed in [4] in the limit of thick wall

$$m \gg e\sqrt{\xi} \,, \tag{83}$$

when the overlap between two edges of the wall is exponentially small.

Now we will discuss the same problem in the opposite limit of a thin wall, with a strong overlap,

$$m \ll e\sqrt{\xi} \,. \tag{84}$$

This limit is usually referred to as the sigma-model limit. If $m \ll e\sqrt{\xi}$, the "photonic" supermultiplet becomes heavy, since the photon mass in the bulk $\sim e\sqrt{\xi}$. Therefore, it can be integrated out, leaving us with the theory of fields from the matter supermultiplets, nearly massless in the scale $e\sqrt{\xi}$, which interact through a nonlinear sigma model with the Kähler term corresponding to the Eguchi–Hanson metric. The manifold parametrized by these (nearly) massless fields is four-dimensional. The two vacua of the model vacua lie at the base of this manifold. Therefore, in considering the domain wall solutions in the sigma-model limit $m \to 0$ [23, 24, 25] one can use the ansatz $q = \tilde{q}^\dagger$ and limit oneself to the base manifold, which is, in fact, a two-dimensional sphere. In this way we arrive at the problem of the domain wall in the CP(1) model deformed by a twisted mass term (related to a non-vanishing $\Delta m = 2m$). In this formulation the problem was first addressed in [24].

In the sigma-model limit one can readily find explicitly the wall profiles,

$$
\begin{aligned}
q^1 &= \bar{\tilde{q}}^1 = \sqrt{\frac{\xi}{2}}\left(\cos\frac{\eta(z)}{2}\right)\,, \\
q^2 &= \bar{\tilde{q}}^2 = \sqrt{\frac{\xi}{2}}\left(\sin\frac{\eta(z)}{2}\right)e^{i\sigma}\,, \\
a &= m\sqrt{2}\left(\sin^2\frac{\eta}{2} - \cos^2\frac{\eta}{2}\right) = -m\sqrt{2}\,\cos\eta\,,
\end{aligned}
\tag{85}
$$

where

$$
\eta(z) = 2\arctan\left(\exp(2mz)\right). \tag{86}
$$

Note that

$$
|q^1|^2 + |q^2|^2 = \xi/2 \tag{87}
$$

for all z. The modulus σ in Eq. (85) reflects the fact that the target space of the CP(1) model with the twisted mass has U(1) symmetry. It is spontaneously broken on each given wall solution. More details on kinks in the CP(1) model with the twisted mass, which appear as domain walls in the problem at hand, can be found in [8].

Since $e^2 \to \infty$ in the sigma-model limit, in the bulk action we can neglect the contribution due to the gauge field strength tensor. The gauge field then becomes non dynamical; it is expressible in terms of the matter fields,

$$
A_\mu = \frac{i\left(\bar{q}\overleftrightarrow{\partial_\mu}\, q - \bar{\tilde{q}}\overleftrightarrow{\partial_\mu}\,\tilde{q}\right)}{\bar{q}q + \bar{\tilde{q}}\tilde{q}}\,. \tag{88}
$$

The scalar field kinetic term tends to zero too, implying

$$
a = \sqrt{2}\,m\,\frac{|q_2|^2 + |\tilde{q}_2|^2 - |q_1|^2 - |\tilde{q}_1|^2}{\bar{q}q + \bar{\tilde{q}}\tilde{q}}\,. \tag{89}
$$

As usual, we promote σ to a (x, y, t)-dependent field on the wall world-volume. In our gauge the field A_z vanishes while the nonvanishing component are

$$
A_k = -2\sin^2\frac{\eta(z)}{2}(\partial_k\sigma)\,, \qquad k = 1, 2\,. \tag{90}
$$

The field strength then takes the form

$$
F_{kz} = \frac{2m}{\cosh^2 2mz}\,(\partial_k\sigma)\,, \qquad k = 1, 2\,. \tag{91}
$$

If we substitute these expressions back in the action, we get

$$S = \int dz\, dt\, d^2x (\partial_k \sigma)^2 \left(\frac{\xi}{2\cosh^2 2mz} + \frac{2m^2}{e^2\, \cosh^4 2mz} \right) , \qquad (92)$$

the the first term is due to the covariant derivative and the second term is due to the field strength tensor. The second term is negligible and can be omitted. This shows that our approximation is self-consistent. Keeping only the first term and integrating over z gives us the normalization of the world-volume effective action,

$$\begin{aligned} S &= \int d^3x\, \beta\, (\partial_k \sigma)^2 \,, \\ \beta &= \int dz\, \frac{\xi}{2\cosh^2 2mz} = \frac{\xi}{2m} \,. \end{aligned} \qquad (93)$$

The σ field is strictly massless, the gauge field that dualizes σ is in the Coulomb phase on the wall world volume.

Quantitatively, the thin wall (sigma model) approximation is not parametrically supported. However, it reveals the existence of a massless modulus on the wall in the most straightforward way. Moreover, it can be conveniently used to discuss a "boojum" configuration, with a flux tube ending on the wall. The approximation is analytic at sufficiently large distances from the point of the wall-tube junction.

The wall-tube junction solution in the sigma-model limit was found (in a different notation) in Refs. [25, 26]. For illustrative purposes we will reproduce it in our notation. The BPS equations for a vortex ending on the wall are (see Ref. [4])

$$\begin{aligned} &B_3 - \frac{g^2}{2}\left(2|q_k|^2 - \xi\right) - \sqrt{2}\partial_3 a = 0 \,, \quad B_1 - iB_2 - \sqrt{2}(\partial_1 - i\partial_2)a = 0 \,, \\ &\nabla_3 q_k = -\frac{1}{\sqrt{2}} q_k (a + \sqrt{2} m_k) \,, \quad (\nabla_1 - i\nabla_2) q_k = 0 \,. \end{aligned} \qquad (94)$$

In the sigma-model limit only q_k's are dynamical variables. Thus, we need to solve two equations in the second line in Eq. (94). This can be done using the following ansatz in the cylindrical coordinates z, r, ϕ:

$$q_1 = \sqrt{\frac{\xi}{2}}\, e^{i\phi}\, \cos\frac{\theta(z,r)}{2} \,, \qquad q_2 = \sqrt{\frac{\xi}{2}}\, \sin\frac{\theta(z,r)}{2} \,. \qquad (95)$$

Then the BPS equations can be written as

$$\frac{\partial\theta}{\partial r} = \frac{1}{r}\sin\theta\,, \qquad \frac{\partial\theta}{\partial z} = 2m\,\sin\theta\,. \tag{96}$$

The solution can be readily found, namely,

$$\theta = 2\arctan\left[\frac{\exp\left(2m(z-z_0)\right)}{r}\right], \tag{97}$$

where z_0 is an integration constant which parametrizes the z position of the object. Now we can use Eqs. (88) and (89) to determine A_μ and a,

$$a = -\sqrt{2}m\cos\theta\,, \qquad A_{\hat{\phi}} = -\frac{\cos^2(\theta/2)}{r}\,. \tag{98}$$

This solution is valid in the sigma-model limit ($m \ll e\sqrt{\xi}$) and at distances $r \gg 1/(e\sqrt{\xi})$ from the point of the wall-tube junction. We see that the gauge field is localized inside the wall and has the Coulomb $1/r$ behavior at large r. This shows that we do have the Coulomb phase on the wall – even in the sigma model limit – and confirms that σ is a strictly massless modulus.

To conclude this section let us return to the gauge theory limit (83) of the problem at hand studied in [4]. One might naively suspect that there are two different moduli fields in the two-flavor model. One is the modulus σ which is exactly massless because it is related to the global U(1) symmetry broken by the wall solution. One might guess that this modulus has nothing to do with the bulk gauge field. Allegedly, the bulk gauge field localized on the wall through the same mechanism as was discussed in the one-flavor model is a quasimodulus $\tilde{\sigma}$ which is different from the modulus σ, and $\tilde{\sigma}$ acquires a small mass due to exponentially small quark fields inside the wall, as in Sect. 3.

The solution for the wall-string junction found in [4] shows that this naive picture is incorrect. In [4] it was shown that the string orthogonal to the domain wall can end on the wall, and the magnetic flux it carries penetrates in the wall. The endpoint of the string plays the role of a vortex for the σ field localized on the wall. In fact, the solution for the wall (far away from the string endpoint) is approximately given by the unperturbed domain wall solution with the collective coordinate σ determined by [4]

$$\sigma \,=\, \alpha, \tag{99}$$

where α is the polar angle on the wall plane. The endpoint of the string creates a vortex of the field σ. This shows that in fact there is no extra field $\tilde{\sigma}$. The gauge field localized on the wall is dual to σ which is strictly massless in the two-flavor model.

5.2 Further discussion of moduli vs. quasimoduli

The example of Sect. 5.1 shows that the two-flavor model has a massless phase field σ localized on the domain wall. This is not related to supersymmetry. Any model with a global U(1) symmetry, two distinct vacua in which the global symmetry is unbroken, and a domain wall that spontaneously breaks this symmetry, automatically has a massless Goldstone boson localized on the domain wall. In particular, the wall solution with $\sigma = \pi$ has the same tension as that with $\sigma = 0$, in an obvious contradistinction with the solution of the toy model discussed in Sect. 3. Note that in the latter case, in the $\sigma = \pi$ wall the matter field vanishes on the plane lying in the middle of the wall. No such zero-plane occurs in the former case.

To better understand the relation between the one- and two-flavor models, we should dwell on the following question: why there is no confinement on the wall in the two-flavor models, although the matter field condensates do not exactly vanish inside the wall? Why the σ field remains massless in this case? A (partial) answer to this puzzling question is as follows. 3+1 dimensional physics inside the wall, between its edges, is not the only thing to consider. Existence vs. nonexistence of a massless modulus is a global effect. The boundary conditions at $z = \pm\infty$ play a crucial role. In the two-flavor model we deal with four phases:

$$q_1(z = -\infty),\ \ q_2(z = -\infty)\ \text{ and }\ q_1(z = +\infty),\ \ q_2(z = +\infty)\,. \tag{100}$$

Moreover,

$$q_1(z = -\infty) \to \sqrt{\frac{\xi}{2}}\,, \quad \text{and}\ \ q_2(z = +\infty) \to \sqrt{\frac{\xi}{2}}\,, \tag{101}$$

while

$$|q_2(z = -\infty)| \to 0\,, \quad |q_1(z = +\infty)| \to 0\,. \tag{102}$$

The massless modulus σ corresponds to a rotation of $q_1(z = -\infty)$ and $q_1(z = +\infty)$ in the same direction while $q_2(z = -\infty)$ and $q_2(z = +\infty)$ remain fixed.

The would-be quasimodulus of Dvali *et al.* corresponds to a rotation of the phases of $q_1(z = +\infty)$ and $q_2(z = +\infty)$ in the same direction while $q_1(z = -\infty)$ and $q_2(z = -\infty)$ remain fixed. The would-be quasimodulus has a tachyonic direction and classically decays into the modulus σ.

Let us try to understand mechanisms responsible for this phenomenon in more detail. Consider a string parallel to the domain wall (a grid of such strings is depicted in Fig. 13). If the distance between the wall and the string

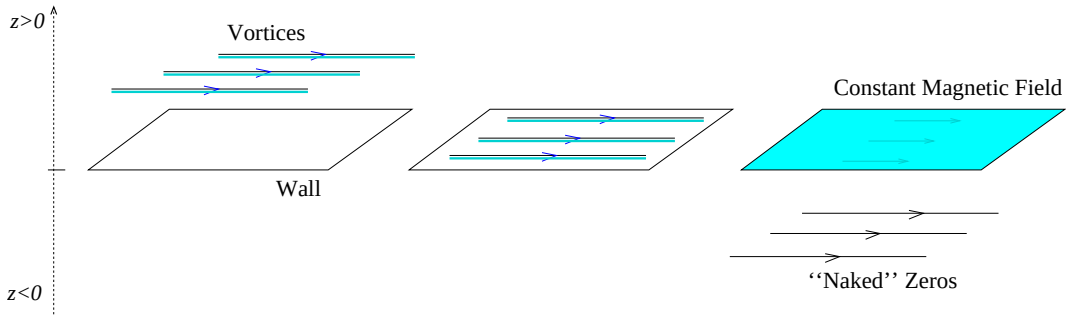

Figure 13: A grid of flux tubes parallel to the domain wall. At $z > 0$ they are made out of the q_2 field condensate. The line of zeroes of the q_2 field is surrounded by the magnetic field. At $z = 0$ the vortices lies in the middle of the wall. Proceeding further the zeroes of q_2 go to z negative while the magnetic field remains on the domain wall surface. In the limit where the zeroes are at $-\infty$ we recover the solution describing a constant magnetic field on the wall.

is very large we have an ordinary ANO string with thickness $\sim 1/(e\sqrt{\xi})$. As we move the string toward the wall, the quark condensate decreases and, in the center of the wall, the thickness of the string (in the directions parallel to the wall) becomes

$$\sim R = \frac{1}{e\sqrt{\xi}e^{-dm/2}}\,, \tag{103}$$

where d is the thickness of the wall. The thickness of the wall depends on the regime in which we find ourselves. In the limit $m/(e\sqrt{\xi}) \gg 1$ the thickness is entirely determined by the matter field and is $d \sim m/(e^2\xi)$. In the opposite limit $m/(e\sqrt{\xi}) \ll 1$ (the sigma-model limit) the thickness is $d \sim 1/m$.

If we want to compare the thickness of the domain wall with that of the string in the middle of the wall we should compare

$$\mathrm{Max}\left[\frac{1}{m}, \frac{m}{e^2\xi}\right]$$

with

$$\frac{1}{e\sqrt{\xi}e^{-dm/2}}\,.$$

Multiplying both sides by $e\sqrt{\xi}$ we can express everything in terms of a dimensionless parameter

$$x = \frac{m}{e\sqrt{\xi}}\,. \tag{104}$$

Thus, we should compare

$$\text{Max}\left[\frac{1}{x}, x\right] \;\text{ with }\; e^{\frac{x^2}{2}}\,.$$

These two functions are plotted in Fig. 14.

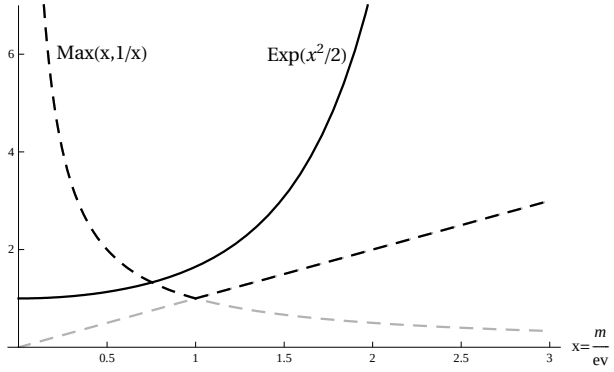

Figure 14: Comparison between the thickness of the domain wall, and the transverse size of the flux tube located inside the domain wall. In the region $x \ll 1$ corresponding to the sigma-model limit, the transverse size of the flux tube is much smaller than the wall thickness.

In the $x \gg 1$ limit the thickness of the string is much larger than the thickness of the domain wall. This is qualitatively consistent with the existence of a Coulomb phase in the middle of the wall. The opposite limit $x \ll 1$ is problematic. The thickness of the string is much smaller than the thickness of the wall. We are thus tempted to conclude that in this regime the wall lives in a confining phase, which is clearly in contradiction with the rigorous proof above of the existence of a massless modulus and, hence, the Coulomb phase.

The way out of this paradox is as follows. In the previous discussion we have compared the thickness of the wall with that of the string in the *middle* of the wall. So we (erroneously) assumed that dynamics on the wall world volume is directly deducible from consideration of 3+1 dimensional dynamics inside the wall, between its two edges. In the $x \gg 0$ limit this creates little problem. In this limit we have a thick region inside the wall in which the matter field condensate essentially vanishes. But in the $x \ll 1$ limit this way of thinking creates a paradox and, thus, reveal its inconsistency.

In fact, the wall world-volume dynamics reflects not only what happens at $z \sim 0$, but also what happens at $z \to \pm\infty$.

Consider a grid of flux tubes at $z > 0$ parallel to the domain wall (Fig. 13). We should remember that $z > 0$ is the region where q_2 condenses while $z < 0$ the region where q_1 condenses. Each flux tube has a line of zeroes for the q_2 field and a magnetic field surrounding this line of zeroes. We then move the grid of flux tubes toward the domain wall. We want to understand what happens to these flux tubes as we pass through the wall and then move toward negative infinity. At $z = 0$ the flux tube grid is in the middle of the wall; the thickness of each flux tube is larger. If we move on, something new happens. The lines of zeroes go to z negative and get separated from their magnetic field. The magnetic field remains trapped inside the wall. In the limit where the zeroes are at $z \to -\infty$, we recover the solution of constant magnetic field inside the domain wall. So, the q_2 flux tube, passing through the wall to the other side of the wall, *does not* become the q_1 flux tube.

This is not in contradiction with the symmetries of the theory. The domain wall is symmetric under the Z_2 transformation $z \leftrightarrow -z$ combined with $q_2 \leftrightarrow q_1$. The one-flavor case is different. The domain wall is symmetric under the parity transformation $z \leftrightarrow -z$ and the q flux tube passing through the wall to the other side of the wall preserves its "identity" remaining the q flux tube.

Of course, physically the line of the q_2 zeroes at $z = -\infty$ (more exactly, the plane of the q_2 zeroes [7]) is in fact not so "far away." The q_2 quark has the exponential profile $\sim \exp\left(-e^2\xi\, z^2\right)$ inside the wall and essentially becomes zero at distances of the order of $1/e\sqrt{\xi}$. Thus, the plane of the q_2 zeroes is shifted from the region where the magnetic field is concentrated by separation of the order of thickness of the flux tube in the vacuum. This is in accord

[7] A flux tube has line of zeroes of a charged scalar inside it, while in order to have a Coulomb phase on the wall we need the whole plane of the q zeroes (parallel to x, y-plane).

with our physical intuition.

Here we arrive at a crucial distinction of the two-flavor model from the one-flavor model of Sect. 2. In the one-flavor model the "empty" domain wall (i.e. without magnetic field) has a nonvanishing Q field everywhere. Inside the wall it becomes small, but still does not vanish. In order for a magnetic field to penetrate the wall we need to have zeroes of the Q-field. Clearly, it costs less energy to create a line of Q-zeroes in the (x, y)-plane than the whole (x, y)-plane of the Q-zeroes. This qualitatively explains why we have confinement on the wall in the one-flavor model (σ is a *quasi*modulus) and the Coulomb phase on the wall in the two-flavor model (σ is strictly massless).

Now, let us discuss energetics of this process. First of all, consider the string grid when it is far away from the wall in the positive-z region. Assume we deal with a homogeneous grid with density f, so that the flux per unit of length is $4\pi f$. The tension of this configuration is the sum of the wall tension plus the string tensions

$$T_{z\gg 0} = \xi\Delta m + 2\pi\xi f\,. \tag{105}$$

In the opposite position, when the zeroes are at negative z, far away from the wall, we can also easily compute the tension. It is just that of a domain wall with a constant magnetic flux inside it. An easy way to get the result is the thin-edge approximation (similar to that adopted in [27] for the Q-wall). The wall tension is now given by a sum of three terms,

$$T\,(d) = \frac{1}{d}\left(\frac{2(\Delta m)^2}{g^2} + \frac{8\pi^2 f^2}{g}\right) + \frac{g^2\xi^2}{8}d\,. \tag{106}$$

Minimizing with respect to d we obtain

$$d = \frac{4}{g^2\,\xi}\left((\Delta m)^2 + 4\pi^2 f^2\right)^{1/2}, \tag{107}$$

and

$$T_{z\ll 0} = \xi\sqrt{(\Delta m)^2 + 4\pi^2 f^2}\,. \tag{108}$$

The expression in Eq. (108) can also be obtained from a more rigorous derivation using the Bogomol'nyi completion method (see Ref. [28]). The physical situation is very similar to the Q-kinks discussed in detail in Refs. [29] for $1+1$ dimensional sigma models. Following [4] we denote

$$q^A = \widetilde{\bar{q}}_A \equiv \frac{1}{\sqrt{2}}\,\varphi^A\,, \tag{109}$$

where we introduce a new complex field φ^A. The action then reduces to

$$\begin{aligned} S_{\rm red} &= \int d^4x \left\{ \frac{1}{4g^2} F_{\mu\nu}^2 + \frac{1}{g^2} |\partial_\mu a|^2 + \bar{\nabla}_\mu \bar{\varphi}_A \nabla_\mu \varphi^A \right. \\ &+ \left. \frac{g^2}{8} \left(|\varphi^A|^2 - \xi \right)^2 + \frac{1}{2} \left|\varphi^A\right|^2 \left| a + \sqrt{2} m_A \right|^2 \right\} . \end{aligned} \tag{110}$$

The Bogomol'nyi completion of the wall+tube energy functional can be written as

$$\begin{aligned} T_{\rm w} = \int dz \quad & \left\{ \left| \cos\alpha \, \nabla_z \varphi^A \pm \frac{1}{\sqrt{2}} \varphi^A (a + \sqrt{2} m_A) \right|^2 \right. \\ & + \left| \sin\alpha \, \nabla_z \varphi^A \mp i \, \nabla_x \varphi^A \right|^2 \\ & + \left| \frac{1}{g} \partial_z a \pm \cos\alpha \, \frac{g}{2\sqrt{2}} (|\varphi^A|^2 - \xi) \right|^2 \\ & + \left| \frac{1}{\sqrt{2} g} \partial_z A_x \pm \sin\alpha \, \frac{g}{2\sqrt{2}} (|\varphi^A|^2 - \xi) \right|^2 \\ & \left. \pm \frac{1}{\sqrt{2}} \cos\alpha \, \xi \partial_z a \pm \frac{1}{2} \sin\alpha \, \xi \partial_z A_x \right\} . \end{aligned} \tag{111}$$

The BPS equations are obtained by putting to zero each of the first four lines of Eq. (111). In order to find an explicit solution, let us choose a gauge where $A_z = 0$; the following ansatz can then be used:

$$\varphi_k = \eta_k(z) \exp(i \lambda_k x) , \qquad a = a(z) , \qquad A_x = -f(z) . \tag{112}$$

From a particular linear combination of the BPS equations we can find the value of λ_k and also that the profile for a and for f are proportional:

$$f(z) = \sqrt{2} \tan\alpha \, a(z) , \qquad \lambda_k = m_k \tan\alpha . \tag{113}$$

The equations for the other profiles give the following first order system:

$$\sqrt{2} \, \partial_z a + \frac{g^2}{2} \cos\alpha (\eta_1^2 + \eta_2^2 - \xi) = 0 , \tag{114}$$

$$\partial_z \eta_k + \frac{1}{\sqrt{2} \cos\alpha} \eta_k (a + \sqrt{2} m_k) = 0 .$$

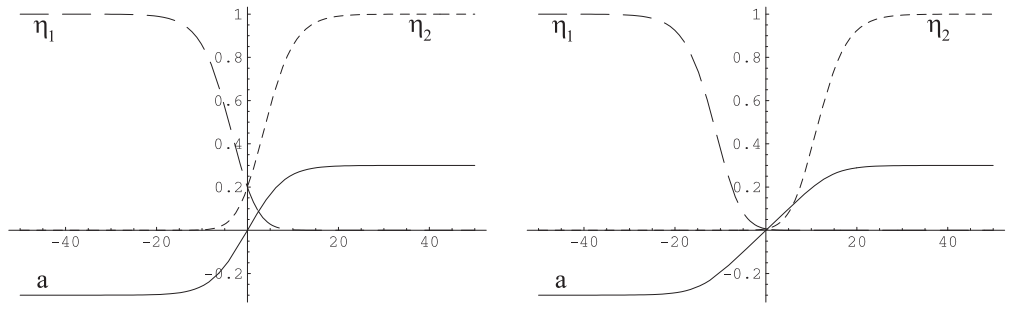

Figure 15: Left: Domain wall without magnetic flux ($\alpha = 0$). Right: Domain wall with magnetic flux ($\alpha = \pi/3$). Due to the magnetic field, the domain wall thickness increases. The following numerical values were used: $m = 0.3$, $e = 0.2$, $\xi = 1$.

A numerical solution is shown in Fig. 15.

For the moment α is an arbitrary angle (this is a usual trick used in analyzing dyons or Q-kinks). The wall+tube boundary conditions are as follows. At $z \to +\infty$

$$\varphi^1 = 0 \ , \quad \varphi^2 = \sqrt{\xi} e^{i2\pi f} \ , \quad A_x = 4\pi f \, . \tag{115}$$

At $z \to -\infty$

$$\varphi^1 = \sqrt{\xi} \ , \quad \varphi^2 = 0 \ , \quad A_x = 0 \, . \tag{116}$$

The decomposition (111) give the upper bound

$$T_{\rm w} \geq \cos\alpha \, \xi \Delta m + \sin\alpha \, 2\pi\xi f \, . \tag{117}$$

Maximizing with respect to α we get exactly the expression in Eq. (108).]

This presents a more quantitative proof of our assertion. The q_2 string parallel to the wall reaches the minimum of the energy when the line of zeroes of q_2 is at $z \to -\infty$, and the tension is given by (108). If, instead, we consider a set of q_1 strings parallel to the wall, the minimum is reached when the line of zeroes of q_1 is at $z \to +\infty$. In both cases the energy is always localized inside the domain wall in the form of a constant magnetic field. The constant magnetic field corresponds to the Coulomb phase on the wall world volume, with the massless modulus $\sigma = ky$.

We can also discuss a different system that will help us to further elucidate these issues. Consider a grid of flux tubes perpendicular to the domain

wall (Fig. 16). The flux tubes are aligned along the z axis and the wall, initially, is aligned in the plane x, y. We assume the flux tubes to be equidistant separated by intervals $1/(2f)$. (We consider twice the density of the previous system for later convenience). Hence, $2f$ is the linear density. The magnetic flux density is $8\pi f$. This simplification will allow us to make computations very quickly. Simultaneously, this set-up still provides us with essential information on physics of the "flux tubes perpendicular to the wall" system.

This flux tube grid, for sufficiently large density $2f$, can be considered as a surface with tension $4\pi\xi f$ and linear flux $8\pi f$. When this surface intersects with the domain wall we have a three-surface junction: the flux tube grid and two semi-planes into which the domain wall is divided. The angle θ shown in Fig. 16 defines geometry of the junction. The magnetic flux carried by the

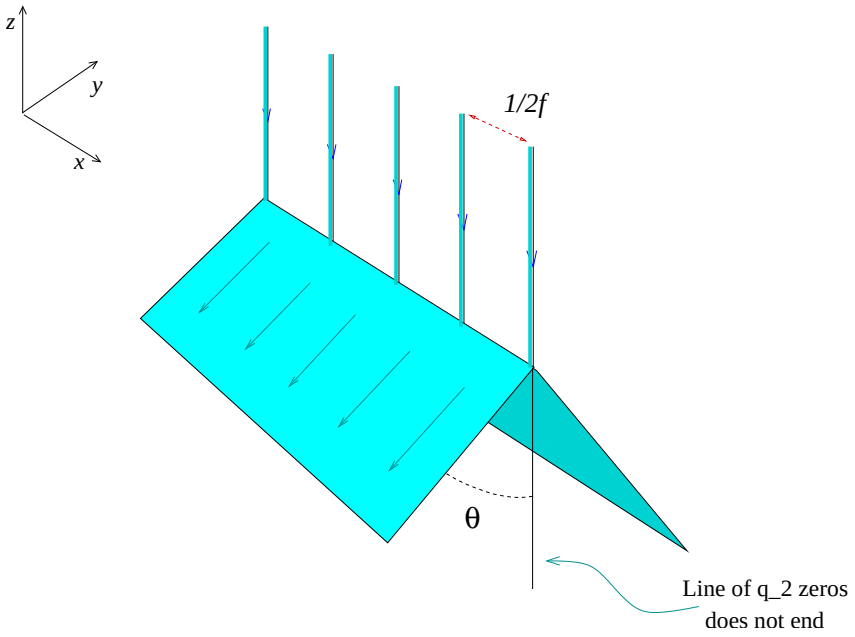

Figure 16: A grid of strings perpendicular to the domain wall. The strings form a linear lattice with distance $1/(2f)$ between them. The domain wall is deformed into the shape shown in this figure in order to balance the tension of the strings. Half flux of the flux tubes goes into each of two semi-planes into which the wall is divided. The angle θ is determined in the text, see Eq. (118). It tends to 0 when the string density $2f$ is very small. It tends to $\pi/2$ when the magnetic flux is very large.

flux tubes is divided exactly into two equal parts, so that each semi-plane carries linear flux $4\pi f$. The wall tension is given by $\xi\sqrt{(\Delta m)^2 + 4\pi^2 f^2}$. The angle θ is determined by a simple balance of tensions,

$$\cos\theta = \frac{2\pi f}{\sqrt{(\Delta m)^2 + 4\pi^2 f^2}}\,. \tag{118}$$

Note that $\theta = \pi/2 - \alpha$ where α is the angle that maximizes the BPS bound (117).

From this simple example we can learn an important lesson. First of all the flux tube grid is a source of a constant magnetic field inside the wall. This means, as was already discussed, that the $2+1$ dimensional theory on the domain wall is in the Coulomb phase. Second, we can conclude that the wall with a constant magnetic field is 1/4 BPS saturated. This follows from the fact that the flux tube perpendicular to the wall is known to be 1/4 BPS (See [4] and Appendix B.) It is straightforward to verify that, if we take the BPS equations for a system of strings ending on the wall (which are in Eq. (94)) and rotate them by an angle α around the x axis, we recover the same equations as those that we get from the Bogomol'nyi completion in Eq. (111).

6 Peculiarities of the Gauge Field Localization. Can we uplift the problem to five dimensions?

As was mentioned in Sect. 2, localization of gauge fields on domain walls is not similar to that of, say, spinor field since dualization is important. This makes the procedure non-local with respect to the gauge potentials in the bulk and on the brane. The latter is not just a mode reduction of the former.

Let us explain it in more detail. To begin with, consider the conventional localization mechanism on topological defects. The bulk theory is defined in space-time X^M where $M = 0, \ldots, d-1$. The soliton is a topological object extended in x^μ where $\mu = 0, \ldots, p$. The transverse coordinates are s^a with $a = p+1, \ldots, d-1$. The theory has some bosonic fields $\phi^{(j)}(x, s)$. The soliton is a topologically stable solution made of the bosonic fields $\phi^{(a)}$ which are independent of x. The soliton is a p-brane spanned on the coordinates x^μ.

Now if we want to find the spectrum of a particular scalar field φ in the soliton background we can separate variables

$$\varphi(x,s) = \sum_n \varphi_\parallel^{(n)}(x)\varphi_\perp^{(n)}(s)\,. \tag{119}$$

In the quadratic in φ approximation the Lagrangian takes the form

$$L = \int d^p x \int d^{d-p}s \left(\partial_M \varphi \partial^M \varphi - f(\phi)\varphi^2\right) \tag{120}$$

implying the following (linear) equations of motion for φ

$$(\partial_M \partial^M + f(\phi))\varphi(X) = 0\,. \tag{121}$$

Inserting here Eq. (119) we get two equations

$$(\partial_a \partial_a + f(\phi))\varphi_\perp^{(n)}(s) \;=\; m_{(n)}^2 \varphi_\perp^{(n)}(s)\,, \tag{122}$$

$$(\partial_\mu \partial^\mu + m_{(n)}^2)\varphi_\parallel^{(n)}(x) \;=\; 0\,, \tag{123}$$

where we used the fact that $\partial_M \partial^M = \partial_\mu \partial^\mu + \partial_a \partial_a$.

The physical meaning of this formula is as follows. First we solve the "transverse" field equation (122) and we find the mass eigenvalues. The corresponding longitudinal field $\varphi_\parallel(x)$ is (generally speaking) a massive field in the longitudinal variables x. As long as $\varphi_\perp^{(n)}$ is normalizable on s^a and $m_{(n)}$ is much smaller than the inverse soliton thickness, we can keep this soliton-localized field in the low-energy Lagrangian emerging on the soliton world volume. For this particle to be massless, the corresponding transverse mode must be a zero mode of the equation (122).

To write the effective Lagrangian for this localized field we use the bulk Lagrangian (120), expand in longitudinal and transverse fields, and integrate over the the transverse variables,

$$\int ds \varphi_\perp(s)^2 \int d^p x \left(\partial_\mu \varphi_\parallel(x)\partial^\mu \varphi_\parallel(x) - m^2 \varphi_\parallel(x)^2\right). \tag{124}$$

The norm of the perpendicular field factorizes out providing a normalization for the parallel field. Only normalizable modes of (122) lead to soliton-localized fluctuations.

Now let us return to gauge fields on 1+2-dimensional walls [4], try to follow the way outlined above and see that this is *not* the right procedure to localize the gauge field.

The bulk fields we start from are the gauge field A_M, and two complex scalar fields q_1 and q_2. The bulk theory is four-dimensional, and q_2. If we want to parallelize the procedure outlined above we "nominate" A_μ ($\mu = 0, 1, 2$) as "our" fields and apply the standard decomposition

$$A_\mu(X) = \varphi_\perp(z) A_\mu(x) \tag{125}$$

(with normalizable $\varphi_\perp$ implying that at $z \to \pm\infty$). Then we note that the magnetic field inside the wall (parallel to the wall) always involves a derivative with over z. The total magnetic flux inside the wall thus contains $\int dz \partial_z \varphi_\perp$ and obviously vanishes.

The mode decomposition (125) is suitable for massive vector fields on the wall. But there is no index theorem that can protect any zero energy solutions of equation (122).

What is the actual procedure leading to the gauge field localization? We must use a global U(1) symmetry (exact in the two-flavor case or approximate in the one flavor case). Spontaneous breaking of this symmetry localizes, through the Goldstone theorem, a phase field on the wall. Dualization of this field gives rise to QED on the wall world volume, with *electric* field directed along the wall. At the same time, the flux *inside* the wall (parallel to the wall) is that of the magnetic field of the original bulk theory.

The necessity of dualization explains why in five- (and higher dimensions) it is so hard to localize gauge fields on the 1+3-dimensional wall within a field-theoretic framework. (By field theory we mean here something without gravity, or at least where gravity does not play essential role in the mechanism of localization.) Such mechanisms could be of enormous phenomenological interest. Ideas as to how one could address this problem can be found in the literature, see e.g. [3, 30, 31].

The construction discussed in the present paper cannot be uplifted to higher dimensions. Let us discuss in more detail what happens if we just lift our four-dimensional models to five dimensions. In four-dimensional theory, what is localized on the 1+2-dimensional wall is a gauge boson

$$F_{ij} = \epsilon_{ijk} \partial_k \sigma \,. \tag{126}$$

where $F_{ij} = \partial_{[i} \widetilde{A}_{j]}$, and $\widetilde{A}_j$ is the localized gauge potential.

As we uplift the model to, say, five dimensions, we observe that what is localized here is not a gauge field but a 2-form, or the Kalb–Ramond filed $\widetilde{H}_{\mu\nu}$. Indeed, now

$$C_{\mu\nu\rho} = \epsilon_{\mu\nu\rho\sigma}\partial_\sigma\sigma\,, \qquad C_{\mu\nu\rho} = \partial_{[\mu}\widetilde{H}_{\nu\rho]}\,. \tag{127}$$

To interpret this result let us ask ourselves what are the sources charged under this Kalb–Ramond field. We know that 2-forms couple naturally to strings, or 1-branes, much in the same way 1-forms couple to particles. We have, in fact, a natural candidate for this string. This is the world sheet spanned by the uplifted ANO vortices ending on the domain wall. The ANO vortices in five dimensions are 2-branes. This is because their codimension is fixed to be 2 from the homotopy $\pi_1(\mathrm{U}(1))$. These ANO vortices (2-branes) end on the domain walls (3-branes), and the intersection between them is exactly the string world sheet, the source of the localized Kalb–Ramond field.

7 Conclusions

Summarizing, we conclude that in certain models a string (flux tube) inside the domain wall is possible. These are the models which we called minimal: in particular, those in which the domain wall interpolates between two vacua where one and the same field condenses. The condensate is exponentially suppressed in the center of the domain wall. A string in the bulk parallel to the domain wall is attracted to the wall. The lowest-energy configuration is achieved when the zeroes of the field are at $z = 0$. Figure 17 illustrates this example. As a result, the U(1) filed trapped on the wall is in the confinement regime.

We compared this regime with that of the two-flavor model. The lowest-energy configuration here is achieved when the zeroes are at $z = -\infty$ (the mirror reflected solution $z \leftrightarrow -z$ is also possible). Now, the Coulomb phase on the wall is energetically preferred to the confining phase (see Fig. 18). Underlying dynamics is not so transparent as in the minimal model, with the "confinement on the wall" regime. Technically the distinction is due to the fact that in the two-flavor model q_1 vanishes on one side of the wall and q_2 on the other, so there is no relative phase between, say, q_1 on the left of the wall and q_1 on the right of the wall. There is only a phase between q_1 on the left and q_2 on the right, and it is not z dependent.

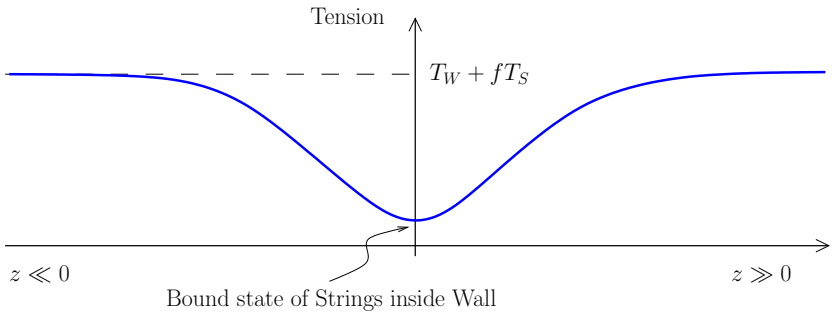

Figure 17: The energy of a string parallel to the wall as a function of the distance in the one-flavor model of Sect. 2 (the minimal model). The string on one side of the wall is the same as the string on the other side. The matter field condensate becomes smaller in the center of the wall; that's why the tension of the string also reaches a minimum at this point. One finds a bound state of string inside the wall.

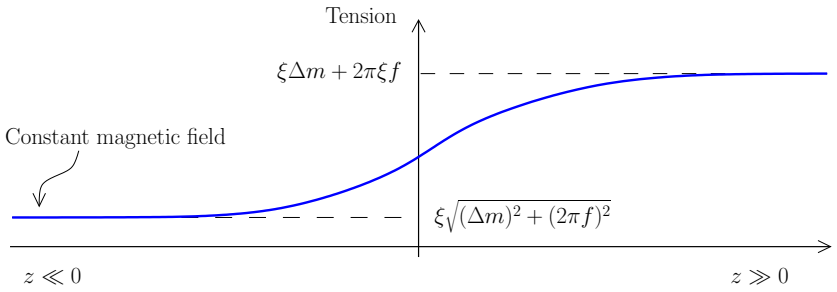

Figure 18: In the two-flavor model discussed in Sect. 4, we consider a domain wall and a set of parallel flux tubes with density f placed at a certain distance z form the wall. At large positive z the tension of this configuration is given by the sum of the tensions of the wall and the grid of the flux tubes. The energy minimum is reached when the distance (defined as the position of the zeroes) is $-\infty$. Then the configuration looks as the domain wall with a constant magnetic field on it.

This technical argument is backed up by an iron-clad symmetry argument. The two-flavor model has a global U(1) in the bulk, which is spontaneously broken on the wall. The Goldstone boson of this breaking is the σ field. It is strictly massless. On the other hand, one can trace its connection to the photon of the bulk theory which is Higgsed in the bulk [4].

The mechanisms we discussed in this paper are quite general. We presented two working examples: a toy minimal model in Sect. 3 and a strong

coupling example in Sect. 4. In both examples there is a condensate which does not vanish in two distinct vacua separated by the domain wall, and a residual (suppressed) condensate in the middle of the wall. The quanta of the fields which condense in both vacua are very heavy inside the wall; hence, one can view the residual condensate as a "tunneling effect" [1].

Acknowledgments

We want to thank G. Dvali for correspondence and useful discussions. R.A. is grateful to FTPI for their hospitality in February 2008 when a part of this work was done. S.B. wants to thank Ki-Myeong Lee and people at KIAS for hospitality extended to him in June 2008 and for interesting discussions. This paper was presented by S.B. at the conference CAQCD-08 in Minneapolis in May 2008.

This work is supported by DOE grant DE-FG02-94ER40823. The work of M.S. was supported in part by *Chaire Internationalle de Recherche Blaise Pascal* de l'Etat et de la Régoin d'Ile-de-France, gérée par la Fondation de l'Ecole Normale Supérieure. The work of A.Y. was supported by FTPI, University of Minnesota, by RFBR Grant No. 09-02-00475a, and by Russian State Grant for Scientific Schools RSGSS-11242003.2.

Appendix A. Vacuum structure

This appendix is devoted to exact computation of the vacuum structure of the theory discussed in Sect. 4 using the technique developed in [19]. The U(2) $\mathcal{N} = 2$ gauge theory, without hypermultiplets, has the following Seiberg–Witten curve

$$\begin{aligned} y^2 &= (z-\phi_1)^2(z-\phi_2)^2 - \Lambda^4 \\ &= (z^2 - u_1 z + \frac{u_1^2}{2} - u_2)^2 - \Lambda^4 \,. \end{aligned} \tag{A.1}$$

The moduli space consists of the Coulomb branch parametrized by $u_1 = \mathrm{Tr}\phi$ and $u_2 = \frac{1}{2}\mathrm{Tr}\phi^2$. The four roots of the curve are

$$\begin{aligned} z^-_{1,2} &= \frac{u_1}{2} \pm \sqrt{-\frac{u_1^2}{4} + u_2 + \Lambda^2} \,, \\ z^+_{1,2} &= \frac{u_1}{2} \pm \sqrt{-\frac{u_1^2}{4} + u_2 - \Lambda^2)} \,. \end{aligned} \tag{A.2}$$

Since we have no hypermultiplets the singularity structure is very simple and consists just of the monopole and dyon singularities (co-dimension 2 surfaces) without intersections

$$u_2 = \frac{u_1^2}{4} \pm \Lambda^2 = 0 \tag{A.3}$$

Now, let us break extended supersymmetry down to $\mathcal{N} = 1$ by virtue of the superpotential

$$W = \alpha \,\mathrm{Tr}\, \left(\frac{\Phi^3}{3} - \xi\Phi \right) . \tag{A.4}$$

Classically, we have the three vacua (36). The quantum solution goes as follows. The Seiberg–Witten curve factorizes,

$$y^2 = P_N^2 - \Lambda^{2N} = F_{2n} H_{N-n}^2 \,, \tag{A.5}$$

where n is the number of the unbroken U(1) factors in the low-energy theory. This factorization is then related to the superpotential parameters,

$$y_m^2 = W_k'^2 + f_{k-1} = F_{2n} \widetilde{Q}_{k-n}^2 \tag{A.6}$$

with

$$\widetilde{Q}_{k-n} = V_{k-N} H_{N-n} + Q_{N-n-1}\,.$$

The unknown parameters are the coefficients of f_{k-1}, the coefficients of V_{k-N} and Q_{N-n-1}, and, finally n parameters of the $\mathrm{U}(1)^n$ Coulomb moduli space. In total $k + n + (k - N) + (N - n - 1) = 2k - 1$, exactly the number of equations from the polynomial equality (A.6).

In the case of interest $N = 2$, $k = 2$ and $n = 1, 2$ depending on whether we deal with the confining vacua or the Coulomb one. The solutions are as follows.

(i) Monopole

We must lie in the monopole singularity

$$u_2 = \frac{u_1^2}{4} + \Lambda^2 = 0\,.$$

On this surface the factorization equation is

$$y_m^2 = (z^2 - \xi)^2 + f_1 = \left(z^2 + -u_1 z + \frac{u_1^2}{4} - \Lambda^2\right)\left(z - \frac{u_1}{2} - a\right)^2\,. \qquad \text{(A.7)}$$

The solution is

$$f_1 = \mp 4\Lambda^2\sqrt{\xi - \Lambda^2}\,z + 4\Lambda^2\xi + 3\Lambda^4 \;\text{ and }\; a = u_1 = \pm 2\sqrt{\xi - \Lambda^2}\,, \qquad \text{(A.8)}$$

where $\pm$ correspond to two classical non-Abelian vacua in Eq. (36).

(ii) Coulomb

The factorization in this case is very simple

$$y_m^2 = (z^2 - \xi)^2 + f_1 = P_2^2 - \Lambda^4\,. \qquad \text{(A.9)}$$

The solution is $u_1 = 0$, $u_2 = \xi$ and $f_1 = -\Lambda^4$. There is no change from the classical formula.

(iii) Dyon

We proceed in the same as above in the monopole case, but now we lie in the singularity

$$u_2 = \frac{u_1^2}{4} - \Lambda^2 = 0\,.$$

The factorization is

$$y_m^2 = (z^2 - \xi)^2 + f_1 = (z^2 + -u_1 z + \frac{u_1^2}{4} + 2\Lambda^2)(z - \frac{u_1}{2} - a)^2\,. \qquad \text{(A.10)}$$

The solution is

$$f_1 = \pm 4\Lambda^2\sqrt{\xi+\Lambda^2}z - 4\Lambda^2\xi + 3\Lambda^4 \;\text{ and }\; a = u_1 = \pm 2\sqrt{\xi+\Lambda^2}\,. \qquad \text{(A.11)}$$

Summarizing, we have five vacua, in total. One is the Coulomb vacuum, whose position in the moduli space is not modified by quantum corrections. Four others are two monopole and two dyon vacua. Their u_2 coordinate is not modified by quantum correction, but the u_1 coordinate is changed. This is why they are aligned in Fig. 6. At the critical value $\xi = \Lambda^2$ the two monopole vacua and the Coulomb vacuum coalesce together. In Sect. 4 we performed our analysis near this critical value, in order to have a low-energy effective action which is weakly coupled on the domain wall profile. Another critical value is at $\xi = -\Lambda^2$ were the dyon vacua coalesce with the Coulomb one.

Appendix B. Comments on supercharges

In this appendix we will show, basing on the central charges, that in $\mathcal{N}=2$ SQED configurations with flux tubes parallel to the domain wall are not BPS saturated. We will follow the formalism of Ref. [4].

The supersymmetry transformations in $\mathcal{N}=2$ SQED are given by the following expressions (where $f,p=1,2$ are $\mathrm{SU}(2)_R$ indices):

$$\begin{aligned}
\delta\lambda^{f\alpha} &= \frac{1}{2}(\sigma_\mu\bar\sigma_\nu\varepsilon^f)^\alpha F_{\mu\nu} + \varepsilon^{\alpha p}D^a(\tau^a)^f_p + i\sqrt{2}\not{\partial}^{\alpha\dot\alpha}\,a\,\bar\varepsilon^f_{\dot\alpha}\,,\\
\delta\psi^{\alpha A} &= i\sqrt{2}\,\not{\nabla}^{\alpha\dot\alpha}q^{fA}\bar\varepsilon_{f\dot\alpha} + \sqrt{2}\varepsilon^{\alpha f}F_f^A\,,\\
\delta\tilde\psi^\alpha_A &= i\sqrt{2}\,\not{\nabla}^{\alpha\dot\alpha}\bar q^f_A\bar\varepsilon_{f\dot\alpha} + \sqrt{2}\varepsilon^{\alpha f}\bar F_{fA}\,,
\end{aligned} \qquad \text{(B.1)}$$

D^a is the $\mathrm{SU}(2)_R$ triplet of D terms:

$$D^1 = i\frac{g^2}{2}\left(|\varphi^A|^2 - \xi\right),\; D^2 = D^3 = 0\,, \qquad \text{(B.2)}$$

while F^f and $\bar F_f$ are the matter F terms,

$$F^{fA} = i\frac{1}{\sqrt{2}}\left(a+\sqrt{2}m_A\right)q^{fA}, \qquad \bar F_{Af} = i\frac{1}{\sqrt{2}}\left(\bar a+\sqrt{2}m_A\right)\bar q_{Af}. \qquad \text{(B.3)}$$

Let us consider a BPS domain wall, oriented in the (x, y) plane. The following supersymmetry transformations are left unbroken by the domain wall:

$$\begin{aligned} \bar{\varepsilon}^2_{\dot{2}} &= -i\varepsilon^{21}, \quad \bar{\varepsilon}^1_{\dot{2}} = -i\varepsilon^{22}, \\ \bar{\varepsilon}^1_{\dot{1}} &= i\varepsilon^{12}, \qquad \bar{\varepsilon}^2_{\dot{1}} = i\varepsilon^{11}. \end{aligned} \tag{B.4}$$

Let us consider a vortex parallel to the z axis. The following supertransformations are left unbroken:

$$\begin{aligned} \varepsilon^{12} = -\varepsilon^{11}\,, \quad \bar{\varepsilon}^2_{\dot{1}} = -\bar{\varepsilon}^1_{\dot{1}}\,, \\ \varepsilon^{21} = \varepsilon^{22}\,, \qquad \bar{\varepsilon}^1_{\dot{2}} = \bar{\varepsilon}^2_{\dot{2}}\,. \end{aligned} \tag{B.5}$$

It is possible then to find a 1/4-BPS soliton corresponding to a vortex perpendicular to the wall, because Eqs. (B.4,B.5) are compatible in the sense that we can solve both constraints taking

$$\begin{aligned} \varepsilon^{12} = -\varepsilon^{11}\,, \\ \varepsilon^{21} = \varepsilon^{22}, \end{aligned} \tag{B.6}$$

and the $\bar{\epsilon}$ given by Eq. (B.4).

Let us then consider a vortex parallel to the y axis. From a simple spinor rotation, we can find supertransformations left unbroken,

$$\begin{aligned} \varepsilon^{12} = -i\varepsilon^{21}\,, \quad \bar{\varepsilon}^2_{\dot{1}} = -i\bar{\varepsilon}^1_{\dot{2}}\,, \\ \varepsilon^{11} = -i\varepsilon^{22}\,, \qquad \bar{\varepsilon}^1_{\dot{1}} = -i\bar{\varepsilon}^2_{\dot{2}}\,. \end{aligned} \tag{B.7}$$

It is easy to check that it is not possible to find a non-trivial solution to the constraints in Eqs. (B.4) and (B.7). This shows that the configuration with the flux tube parallel to the domain wall breaks all supersymmetries of the theory.

Let us then consider a domain wall in the (x, y) plane with some constant magnetic field along the x axis. As discussed in Figure 16, the unbroken supercharges are the same of the system of a vortex ending on a wall (modulo a rotation by the angle in Eq. (118) along the y axis).

References

[1] G. R. Dvali and M. A. Shifman, Phys. Lett. B **396**, 64 (1997) [Erratum-ibid. B **407**, 452 (1997)] [arXiv:hep-th/9612128].

[2] B. S. Acharya and C. Vafa, arXiv:hep-th/0103011.

[3] S. L. Dubovsky and V. A. Rubakov, Int. J. Mod. Phys. A **16**, 4331 (2001) [arXiv:hep-th/0105243].

[4] M. Shifman and A. Yung, Phys. Rev. D **67**, 125007 (2003) [arXiv:hep-th/0212293].

[5] R. Auzzi, M. Shifman and A. Yung, Phys. Rev. D **74**, 045007 (2006) [arXiv:hep-th/0606060].

[6] G. Dvali, H. B. Nielsen and N. Tetradis, Phys. Rev. D **77**, 085005 (2008) [arXiv:0710.5051 [hep-th]].

[7] A. M. Polyakov, Nucl. Phys. B **120**, 429 (1977).

[8] M. Shifman and A. Yung, Rev. Mod. Phys. **79**, 1139 (2007) [arXiv:hep-th/0703267].

[9] D. Tong, arXiv:hep-th/0509216.

[10] M. Eto, Y. Isozumi, M. Nitta, K. Ohashi and N. Sakai, J. Phys. A **39** (2006) R315 [arXiv:hep-th/0602170].

[11] G. 't Hooft, Nucl. Phys. B **79**, 276 (1974); A. M. Polyakov, JETP Lett. **20**, 194 (1974) [reprinted in *Solitons and Particles*, Eds. C. Rebbi and G. Soliani, (World Scientific, Singapore, 1985), p. 522].

[12] A. Abrikosov, Sov. Phys. JETP **32** 1442 (1957) [Reprinted in *Solitons and Particles*, Eds. C. Rebbi and G. Soliani (World Scientific, Singapore, 1984), p. 356]; H. Nielsen and P. Olesen, Nucl. Phys. **B61** 45 (1973) [Reprinted in *Solitons and Particles*, Eds. C. Rebbi and G. Soliani (World Scientific, Singapore, 1984), p. 365].

[13] N. Seiberg and E. Witten, Nucl. Phys. B **426**, 19 (1994) [Erratum-ibid. B **430**, 485 (1994)] [arXiv:hep-th/9407087].

[14] R. Jackiw and C. Rebbi, Phys. Rev. D **13**, 3398 (1976).

[15] J. E. Kiskis, Phys. Rev. D **15**, 2329 (1977); M. M. Ansourian, Phys. Lett. B **70**, 301 (1977); N. K. Nielsen and B. Schroer, Nucl. Phys. B **120**, 62 (1977); R. Jackiw and P. Rossi, Nucl. Phys. B **190**, 681 (1981); E. J. Weinberg, Phys. Rev. D **24**, 2669 (1981).

[16] A. Gorsky, M. Shifman and A. Yung, Phys. Rev. D **75**, 065032 (2007) [arXiv:hep-th/0701040].

[17] I. I. Balitsky and A. V. Yung, Phys. Lett. B **168**, 113 (1986).

[18] F. Cachazo, M. R. Douglas, N. Seiberg and E. Witten, JHEP **0212** (2002) 071 [arXiv:hep-th/0211170].

[19] F. Cachazo, N. Seiberg and E. Witten, JHEP **0302**, 042 (2003) [arXiv:hep-th/0301006];

[20] V. S. Kaplunovsky, J. Sonnenschein and S. Yankielowicz, Nucl. Phys. B **552** (1999) 209 [arXiv:hep-th/9811195].

[21] R. Portugues and P. K. Townsend, Phys. Lett. B **530**, 227 (2002) [arXiv:hep-th/0112077].

[22] B. Chibisov and M. A. Shifman, Phys. Rev. D **56** (1997) 7990 [Erratum-ibid. D **58** (1998) 109901] [arXiv:hep-th/9706141].

[23] J. P. Gauntlett, D. Tong and P. K. Townsend, Phys. Rev. D **64**, 025010 (2001) [hep-th/0012178].

[24] D. Tong, Phys. Rev. D **66**, 025013 (2002) [hep-th/0202012].

[25] J. P. Gauntlett, R. Portugues, D. Tong and P. K. Townsend, Phys. Rev. D **63**, 085002 (2001) [arXiv:hep-th/0008221].

[26] Y. Isozumi, M. Nitta, K. Ohashi and N. Sakai, Phys. Rev. D **71**, 065018 (2005) [arXiv:hep-th/0405129].

[27] S. Bolognesi and M. Shifman, Phys. Rev. D **76**, 125024 (2007) [arXiv:0705.0379 [hep-th]].

[28] E. Bogomol'nyi, *The stability of classical solutions,* Sov. J. Nucl. Phys. **24**, 449 (1976) [Reprinted in *Solitons and Particles*, Eds. C. Rebbi and G. Soliani (World Scientific, Singapore, 1984), p. 389].

[29] E. R. C. Abraham and P. K. Townsend, Phys. Lett. B **291** (1992) 85; E. R. C. Abraham and P. K. Townsend, Phys. Lett. B **295** (1992) 225.

[30] S. L. Dubovsky, V. A. Rubakov and S. M. Sibiryakov, JHEP **0201**, 037 (2002) [arXiv:hep-th/0201025].

[31] Y. Isozumi, K. Ohashi and N. Sakai, JHEP **0311**, 061 (2003) [arXiv:hep-th/0310130]; JHEP **0311**, 060 (2003) [arXiv:hep-th/0310189].